Computational and Structural Biotechnology Journal 19 (2021) 880–896

COMPUTATIONAL AND STRUCTURAL BIOTECHNOLOGY JOURNAL

journal homepage: www.elsevier.com/locate/csbj

The impact of episporic modification of *Lichtheimia corymbifera* on virulence and interaction with phagocytes

Mohamed I. Abdelwahab Hassan [a,b,c], Monique Keller [b], Michael Hillger [b], Ulrike Binder [d], Stefanie Reuter [e,k], Kristina Herold [e], Anusha Telagathoti [a,1], Hans-Martin Dahse [a], Saiedeh Wicht [f], Nora Trinks [f], Sandor Nietzsche [g], Tanja Deckert-Gaudig [h], Volker Deckert [h,i,j], Ralf Mrowka [e,k], Ulrich Terpitz [f], Hans Peter Saluz [a], Kerstin Voigt [a,b,*]

[a] *Leibniz Institute for Natural Product Research and Infection Biology – Hans Knöll Institute (HKI), Jena, Germany*
[b] *Institute of Microbiology, Friedrich Schiller University Jena, Jena, Germany*
[c] *Pests & Plant Protection Department, National Research Centre, 33rd El Buhouth St. (Postal code: 12622) Dokki, Giza, Egypt*
[d] *Department of Hygiene, Microbiology and Public Health, Institute of Hygiene and Medical Microbiology, Medical University Innsbruck, Schöpfstrasse 41/2, 6020 Innsbruck, Tirol, Austria*
[e] *Experimental Nephrology Group, KIM III, Universitätsklinikum Jena, Jena, Germany*
[f] *Department of Biotechnology and Biophysics, Julius Maximilian University of Würzburg, Biocenter - Am Hubland, Würzburg, Germany*
[g] *Elektronenmikroskopisches Zentrum, Universitätsklinikum Jena, Jena, Germany*
[h] *Leibniz Institute of Photonic Technology (IPHT), Albert-Einstein-Str. 9, 07745 Jena, Germany*
[i] *Institute of Physical Chemistry and Abbe Center of Photonics, Friedrich-Schiller University, Helmholtzweg 4, 07743 Jena, Germany*
[j] *Institute of Quantum Science and Engineering, Texas A&M University, College Station, TX 77843-4242, USA*
[k] *ThIMEDOP-Thüringer Innovationszentrum für Medizintechnik-Lösungen, Universitätsklinikum Jena, Jena, Germany*

ARTICLE INFO

Article history:
Received 17 November 2020
Received in revised form 12 January 2021
Accepted 14 January 2021
Available online 20 January 2021

Keywords:
Monocytes
Intracellular survival
Galleria mellonella
Hyperspectral imaging (HIS)
Atomic Force Microscopy (AFM)
Transmission Electron Microscopy (TEM)

ABSTRACT

Fungal infections caused by the ancient lineage Mucorales are emerging and increasingly reported in humans. Comprehensive surveys on promising attributes from a multitude of possible virulence factors are limited and so far, focused on *Mucor* and *Rhizopus*. This study addresses a systematic approach to monitor phagocytosis after physical and enzymatic modification of the outer spore wall of *Lichtheimia corymbifera*, one of the major causative agents of mucormycosis. Episporic modifications were performed and their consequences on phagocytosis, intracellular survival and virulence by murine alveolar macrophages and in an invertebrate infection model were elucidated. While depletion of lipids did not affect the phagocytosis of both strains, delipidation led to attenuation of LCA strain but appears to be dispensable for infection with LCV strain in the settings used in this study. Combined glucano-proteolytic treatment was necessary to achieve a significant decrease of virulence of the LCV strain in *Galleria mellonella* during maintenance of the full potential for spore germination as shown by a novel automated germination assay. Proteolytic and glucanolytic treatments largely increased phagocytosis compared to alive resting and swollen spores. Whilst resting spores barely (1–2%) fuse to lysosomes after invagination in to phagosomes, spore trypsinization led to a 10-fold increase of phagolysosomal fusion as measured by intracellular acidification. This is the first report of a polyphasic measurement of the consequences of episporic modification of a mucormycotic pathogen in spore germination, spore surface ultrastructure, phagocytosis, stimulation of Toll-like receptors (TLRs), phagolysosomal fusion and intracellular acidification, apoptosis, generation of reactive oxygen species (ROS) and virulence.

Abbreviations: AFM, Atomic Force Microscopy; CD14, Cluster of differentiation 14; CFW, Calcofluor white; HEK, human embryonic kidney; HSI, Hyperspectral imaging; IPS, Insect physiological saline; LCA, *Lichtheimia corymbifera* attenuated; LCV, *Lichtheimia corymbifera* virulent; MD-2, Myeloid Differentiation factor 2; MH-S, Murine alveolar macrophages; MM6, Acute monocytic leukemia derived human monocyte Mono-Mac-6; NF-κB, Nuclear factor 'kappa-light-chain-enhancer' of activated B-cells; PBS, Phosphate buffer saline solution; PI, Phagocytosis index; ROS, Reactive oxygen species; TEM, Transmission Electron Microscopy; TLRs, Toll like receptors.

* Corresponding author at: Leibniz Institute for Natural Product Research and Infection Biology - Hans Knöll Institute (HKI), Jena Microbial Resource Collection, Adolf-Reichwein-Str. 23, 07745 Jena, Germany.
E-mail address: kerstin.voigt@leibniz-hki.de (K. Voigt).
[1] Present address: University Innsbruck, Institute of Microbiology, Technikerstr. 25, 6020 Innsbruck, Austria.

https://doi.org/10.1016/j.csbj.2021.01.023

1. Introduction

Mucormycosis is a life-threatening disease particular for patients that suffer from immunodeficiency [1]. Various species of mucoralean fungi cause mucormycosis such as *Rhizopus, Lichtheimia,* and *Mucor*. Though, the mortality rate caused by mucormycosis is increasing tremendously during the last decades, especially in the developing countries [1]. Knowledge on the interaction of mucoralean fungi with immune system is still marginal [2–4]. The first histologically proven case of mucormycosis (Mycosis mucorina) was reported by Platauf at the University of Graz in 1885 [5]. This first case of disseminated disease in a cancer patient was caused by *Absidia corymbifera* (current name: *Lichtheimia corymbifera*) [6,7]. Since the past decades, infections caused by *Lichtheimia* species are emerging. These infections often develop rapidly, predominantly with rhinocerebral and pulmonary manifestations, and are often associated with dissemination and high mortality rates [8].

Among species causing mucormycosis, *Lichtheimia* species rank the second and third in Europe and USA, respectively [8]. The genus *Lichtheimia* comprises six species namely *L. corymbifera*, *L. ramosa*, and *L. ornata* that are virulent and *L. hyalospora*, *L. sphaerocystis*, and *L. brasiliensis* that are not virulent in clinical settings [9]. The innate immune system is the first line of defence in human against fungi entering the lung. Alveolar macrophages play a key role in the innate immune system in the lung as they are main weapon in eradicating the foreign particles [10]. Therefore, we postulate that the surface structure of the cell wall of *Lichtheimia* spores plays a crucial role during host-pathogen interaction.

In addition to human predispositions, also some fungal characteristics have to comply with the requirements for infection [11]. Such virulence factors also include surface attributes of the spores as infectious agents.

Various studies showed the importance of surface structures of the cell wall of Mucorales during the interaction with host cells such as the spore coat protein (CotH) [2] that is present on the surface of *Rhizopus oryzae* spores, counts as a virulence factor and has a role in invasion process and eumelanin that play a central role in blocking the phagosome maturation in murine macrophages [12].

Initial studies investigated the role of surface and secreted proteins in the pathogenesis of mucoralean fungi such as in *Mucor. circinelloides* [13]. However to the best of our knowledge, there are no studies available which report the role of the spore wall during the interaction with macrophages as major players of innate immune system in *Lichtheimia*. Therefore, the aim of this study is to explore the influence of the spore wall on phagocytosis and acidification process during interaction with macrophage cells, besides testing their role in the pathogenicity through virulence potential in the *Galleria mellonella* model [14]. For this, the outer layer of the sporangiospores (spores released from the sporangium), which is traditionally named epispore, is systematically shaved layer by layer with different physical and enzymatic treatments. Moreover, the current study investigated the effect of the spores of *L. corymbifera* on apoptosis process, and generation of reactive oxygen species by macrophages during the host-pathogen interaction.

2. Material and methods

2.1. Fungal strains, cultivation

Two strains of *Lichtheimia corymbifera* were used in this study: JMRC:FSU:09682, which is referred to virulent *L. corymbifera* (LCV), and JMRC:FSU: 10164, which is referred to attenuated *L. corymbifera* (LCA) as revealed by avian and murine infection models prior to this [15,16]. Cultivation was performed in KK1 minimal medium (10 g glucose, 3 g KH_2PO_4, 1.25 g K_2HPO_4, 0.5 g $MgSO_4{\cdot}7H_2O$, 2 g yeast extract, 1 g KNO_3, 0.5 g KCl, and 4.4 g NaCl dissolved in 1 L of distilled water) or in supplemented minimal medium (SUP: 10 g glucose, 4 g KH_2PO_4, 0.9 g K_2HPO_4, 0.25 g $MgSO_4{\cdot}7H_2O$, 1 g NH_4Cl, and 5 g yeast extract dissolved in 1 L of distilled water) or malt extract agar medium (MA) (30 g malt extract media and 14 g agar dissolved in 1 L of distilled water). The all chemicals that were used in the current study were manufactured by Carl Roth, Germany.

2.2. Cell cultivation, cell viability and induction of apoptosis

All cells were incubated at 37 °C in a humidified incubator with 5% (v/v) CO_2. The murine alveolar macrophage cell line MH-S (MH-S ATCC ® CRL-2019™ *Mus musculus* lung) was primarily used for all cell-spore interaction experiments. MH-S cells were maintained in RPMI-1640 medium (Lonza, BE12-16F supplemented with 10% (v/v) heat-inactivated fetal bovine serum (FCS, Thermo Fisher Scientific, ATCC-30–2020), 1% (w/v) sodium bicarbonate (Lonza, Köln, Germany), and 0.05 mM β-mercaptoethanol (Life Technologies, Darmstadt, Germany). MH-S macrophages were cultivated in cell culture flasks (Sarstedt T25) and subsequently seeded on glass cover-slips in 24- well plates (NUNC, 142475) with 2×10^5 macrophage cells were seeded for each well and subsequently incubated overnight for adherance. For spatio-temporal measurements of the intracellular pH by Hyper Spectral Imaging technique [17], the acute monocytic leukemia derived human monocyte Mono-Mac-6 (MM6, CVCL_1426, ThermoFisher) cell line was used due to their ability to be in suspension. MM6 cells were cultivated using RPMI-1640 (Life technologies, Darmstadt, Germany) complemented with 10% (v/v) heat-inactivated fetal calf serum (FCS) (Lonza, Verviers, Belgium), 2 mM L-glutamine (Lonza, Wuppertal, Germany), MEM non-essential amino acids (PAA Laboratories GmbH, Cölbe, Germany), 1 mM sodium pyruvate (Lonza, Wuppertal, Germany), 10 μg/ml human insulin (Sigma-Aldrich, Germany),10 mg/ml gentamicin (PAA Laboratories GmbH, Cölbe, Germany). The cells were washed with RPMI-1640 medium, seeded out at approximately 1×10^6 cells/75 cm^2 flask and passaged at a 1:3 ratio twice a week. The cell viability was measured before each assay using Trypan Blue Dye 0.4% (w/v) (Bio-Rad Laboratories, USA). To calculate the percentage of live cells, trypan blue dye and cell suspension were mixed in a 1:1 ratio and incubated for 6 min at room temperature, loaded into the counting slides (dual chamber for cell counter; Bio-Rad Laboratories, USA) and then measured in Bio-Rad TC10™ automated cell counter. For induction of apoptosis in monocytes, MM6 cells were seeded at 1×10^6 cells/ml in a six- well plate in complete RPMI-1640 FCS-free medium. Staurosporine (AppliChem, A7626) (1 mM in DMSO) (Carl Roth, Karlsruhe, Germany) was added to a final concentration of 1.5 μM and incubated at 37 °C and 5% (v/v) CO_2 for 1 h.

2.3. Spore harvest and treatments

Resting spores were harvested from 7 days old fully mycelia grown on agar plates at 37 °C with 5 ml of phosphate buffered saline (PBS) that is composed of: 8 g NaCl, 0.2 g KCl, 1.44 g Na_2HPO_4, and 0.2 g KH_2PO_4 dissolved in 1 L of distilled water at pH 7.4. Spores were collected by centrifugation at 6300*g* for 3 min Swelling was carried out by incubation of freshly harvested resting spores in RPMI-1640 medium for 3 h at 37 °C. For opsonization, the spores were coincubated with 500 μl either in murine serum (Sigma-Aldrich, NS03L) or human serum (Sigma-Aldrich, H4522) from clotted human male whole blood under constant gentle shaking at 37 °C for 30 min. Sera inactivated at 65 °C for 30 min were used as negative controls of opsonization. The following enzymatic treatments were performed in PBS: For glucanolytic treatment the

resting spores were incubated in 0.07 g/ml Vinotaste (NovozymesPro, 250G), for specific *endo*-β-1.3-endoglucanolytic treatment with 0.05 g/ml kitalase (Wako Chemicals, 118–00371, for proteolytic treatment with 1 mg/ml pronase E (Protease from *Streptomyces griseus*, Sigma-Aldrich, P5147). The pronase E solution was predigested at 50 °C for one hour prior application. For surface protein modification and removal of modifying groups of proteins, resting spores were trypsinized with 12.5 μg/ml trypsin (from Bovine Pancreas, Sigma-Aldrich) in 25 mM ammonium bicarbonate buffer at pH 7.8 (800 μl per 10^8 spores) and incubated for 30 min at 37 °C with gently shaking. For lipolytic treatment, the resting spores were incubated in 1 ml PBS supplemented with 0.1 ml Tween 20 (Roth, 9127.1). For heat- and UV-inactivation, the resting spores were heated in boiling water bath at 37 °C for 90 min or subjected to UV irradiation on a transilluminator at 321 nm wavelengths for 90 min, respectively. If not stated otherwise, for all treatments spores were incubated for 90 min under gentle shaking at 37 °C after the treatment spores were washed three times with PBS followed by iterative steps of centrifugation at 6300*g* for 3 min, discarding of the supernatant and dissolving of the spores in 1 ml of PBS. Staining the treated spores with FITC was conducted as following: 1 ml of PBS containing treated spores were mixed with 3.5 ml PBS at pH 7.4, 0.5 ml 0.1 M Na_2CO_3 and 0.5–1.0 ml 0.1 mg/ml FITC (Fluorescein isothiocyanate; Sigma-Aldrich Chemie GmbH, F-3651) and subsequently incubated for 30 min under gentle shaking at 37 °C. The spores were collected by centrifugation at 6300*g* for 5 min and washed at least twice or until the supernatant became clear. The spore pellets were resuspended in 1 ml PBS, filtered through Easy strainer filter (40 μm-sterile, Greiner Bio-one) to remove any residual hyphal debris. Spores were counted after the treatments in order to ensure equal spore concentrations for accurate comparison. The spore concentration was determined by mixing 10 μl of the filtrated spore solution with 990 μl PBS pH 7.4 and application to a Thoma chamber. Spores were diluted in RPMI-1640 to a final concentration of 10^6 spore/ml and immediately confronted with 2×10^5 macrophage cells.

2.4. Quantification of phagocytosis and time course of engulfment of L. corymbifera spores by murine alveolar macrophages

MH-S cells (2×10^5 cells/well) were liberated from the RPMI-1640 medium by gentle pipetting and confronted with pre-warmed RPMI-1640 medium containing 1×10^6 spores to a final concentration multiplicity of infection MOI of 5. The co-infection plate was centrifuged at 100*g* for 5 min at room temperature and incubated for 3 h at 37 °C in a humidified 5% (v/v) CO_2 incubator. After incubation, the phagocytosis reaction was stopped by washing with ice-cold PBS twice. Spores that were not phagocytosed were stained with 0.5 mg/ml calcofluor white (CFW; Sigma-Aldrich, F3543) in PBS at pH 7.4 for 15 min at room temperature. The cells were washed twice with PBS, then fixed with 3.7% (v/v) formaldehyde (Roth, 4979) dissolved in PBS for 15 min at room temperature and finally the cells were washed twice with PBS. Before mounting the coverslips onto the glass slides, one drop Roti®-mount fluorcare (ROTH, HP20.1) was applied as anti-fading to increase the resolution for microscopic examination by using a BX-51M (Olympus, Hamburg) at a magnification of 40x using bright field or fluorescence with filterset1 (Excitation 488 nm/ Emission. 510 nm, green) for phagocytosed spores and filterset2 (Excitation. 550 nm/Emission. 610 nm, blue) for detection non-phagocytosed spores. For every cover slide ten images were scanned for each treated spores. In order to distinguish between spores inside and outside macrophages, bright field and fluorescence images (blue and green channel) were overlaid for the same area by using ImageJ [16]. A total of ten overlay images for each sample were subjected to determine the phagocytosis index (PI) manually. Briefly, the number of macrophage with spores and the number of macrophages without spores were counted. The calculation of the percentage of uptake was performed through the following equation that is denoted as (A):

$$\frac{\text{Number of phagocytosed macrophges} * 100}{\text{Number of phagocytosed macrophages} + \text{Number of non - phagocytosed macrophages}}$$

Macrophages were sorted to different categories according to the number of engulfed spores per macrophages (1, 2, 3, and etc.). The number of macrophage cells that participated in the phagocytosis process was multiplied by the number of engulfed spores that is denoted (B). The sum of (B) was divided by the total number of macrophages with spores as determined during the first step. The resulting quotient (C) refers to the average macrophage count per engulfed spore. Finally, the phagocytosis index results from multiplication of (A) value by (C).

2.5. Time course of spore germination

Spore germination was elucidated by end-point and time-lapse-assisted measurements. For end-point measurement, 2×10^3 resting and treated spores of LCV and LCA strains (5 μl spore suspension, spore concentration 4×10^5 spores/ml) were seeded in 100 μl SUP medium on slides and kept at 37 °C in a moist chamber to reduce desiccation. The number of germinated spores was determined by microscopic imaging (Moticam 5.0 MP) every hour between 3 and 6 h of incubation. One-hundred spores per replicate were counted with ImageJ. A total of three biological replicates, each in three technical replicates were carried out.

For time-lapse-assisted measurements, spores were spread in 0.005% (w/v) poly-D-lysine coated 8-well chambers (about 3×10^4- spores/well) and incubated for 15 min at 37 °C to ensure sedimentation of the spores. Spore germination was recorded as time-lapse in KK1-medium for 15 h (1 frame/5 min). Data recording was done by an EVOS2 microscope (Thermo Fisher Scientific) with 20-fold magnification in a heat-controlled chamber at 37 °C. If required, frame-shift correction was performed using the ImageJ macro HyphaTracker [18,19].

2.6. Measurement of intracellular acidification indicating phagolysosomal fusion

Intracellular acidification was elucidated by end-point and Hyperspectral Imaging Microscopy (HSI)-assisted measurements.

2.6.1. End-point measurement

2×10^5 macrophage cells per well were pre-incubated with LysoTracker™ Red DND-99 (Thermofisher, L7528) for 30 min at 37 °C incubator implemented with 5% (v/v) CO_2. 10^6 resting and modified spores of LCV and LCA strains of *L. corymbifera* were co-incubated with MH-S cells after synchronization step (100*g*, 5 min, at room temperature) for 3 h at 37 °C under 5% (v/v) CO_2. The non-phagocytosed spores were removed by repeating extensive washing step three times by RPMI-1640 medium. Co-incubating the heat-killed spores with MH-S cells considers as positive control. For chloroquine treatment, macrophage cells were pre-incubated with 20 μg/ml for one hour at 37 °C before LysoTracker staining. The acidification was monitored after five different time points (3, 6, 8, 18, and 24) hours using LSM-5 LIVE confocal laser scanning microscopy. The percentage of acidification was calculated by determining how many spores were acidified out of at least two hundred phagocytosed spores. Three independent biological replicates were performed.

2.6.2. HSI- measurements

The spores were labeled with a dye mixture containing 1 μl of 1 mg/ml of pHrodo™ Red, succinimidyl ester [(pHrodo™ Red, SE; stock solution 10 mM in DMSO), 6.5 μl of DMSO, 4 μl of 0.1 M $NaHCO_3$ freshly prepared, and 1 μl pH ~ 6] incubated for 30–45 min at room temperature in the dark. After incubation, the spores were washed with 1:10 ratio of DMSO twice and one time with HBSS (Hank's Balanced Salt Solution, Life technologies, Darmstadt, Germany) until the solution was colorless. Monocytes of the cell line MM6 were co-incubated with spores MOI = 3 in FCS/phenol red-free RPMI-1640 medium (Thermo Fischer, 11875085) at 37 °C under 5% (v/v) CO_2 for 1 h. Engulfment was checked using light microscopy (Zeiss, Germany) and 80 μl sample was then loaded on the μ-slide $VI^{0.4}$ microchannel (ibidi GmbH, Martinsried, Germany) to fix cells and refresh media from time to time. HSI-microscopy was performed over a period of 48 h as described previously [17]. The hyper spectral imaging equipment consisted of a built-in camera attached to an imaging spectrograph, a microscope connected to a PCO Sensicam 680KU supplied by a sensitive Electron Multiplying Charge Coupled Device (EMCCD) sensor and to a heating stage which controls the temperature on the stage to avoid medium evaporation [17] The HSI unit was connected to a side port of inverse fluorescence microscope Nikon Diaphot TMD camera with an adapter. The fluorescence was excited by a Nikon epi fluorescence attachment TMD EF supplied by a mercury arc lamp. To detect the pHrodo red signal, the filter cassette DM580 (excitation EX 510 to 560) was used. All the microscopic images were taken from SLR camera (Nikon D600) attached to the front camera port of the microscope. In single cell measurements, the entire spectrum was obtained from the signal emitted by the fluorescent dye [17] The wavelength (horizontally) was plotted against the signal intensity containing the fluorescence emission resolved in space (vertically) to give the entire spectrum graphically. The obtained spectra from the measurements were then processed by the ImageJ software resulting in the raw data. The extracted raw data was converted into the readable digits (smoothened) by python [20]. The signal intensity of the infected cells was then co-related with the signal intensities of the pH buffers to understand the acidic pattern of the cell. The data was plotted as time *vs* signal intensities on the primary y-axis and pH on the secondary y-axis which was derived using generalized linear model (glm) function in R programming (version 4) (https://www.r-project.org/). The model we used as follows: pH = −7.11 + 0.004 × intensity. Also, to prevent the background noise in the signals the data was smoothened using spline approximation [21].

2.7. Effect of L. corymbifera spores on the apoptosis of MH-S cells

The apoptosis measurements were carried out according to Volling et al. (2007) with minor modifications [22]: 2×10^5 MH-S cells were cultivated on 24-well plates and incubated overnight at 37 °C under 5% (v/v) CO_2 incubation chamber for adherence. 10^6 resting, heat-killed, and UV-treated spores from LCV and LCA strains of *L. corymbifera* were co-incubated with MH-S for 3 h at 37 °C at 5% (v/v) CO_2. MH-S cells were washed three times to remove any excess of adherent spores and incubated with 1.5 μM staurosporine (AppliChem, Darmstadt, Germany, A7626) for 16 h to induce apoptosis. The media were removed and the remaining MH-S cells were co-incubated with FITC annexin-V (BioLegend, 640906) and with fixable viability Dye eFluor™ (Thermofisher, 780 65-0865-14) for 15 min in the dark at 4 °C to determine the percentages of apoptotic and necrotic macrophage cells, respectively by flow cytometry (Becton Dickinson LSRII). Three independent biological replicates were conducted.

2.8. Reactive oxygen species measurement

Reactive oxygen species (ROS) were determined as described previously [23]: 4×10^4 MH-S cells were cultivated on 96- well plates at 37 °C under 5% (v/v) CO_2 overnight for adherence. 2×10^5 resting, heat-killed, and UV-killed spores of LCV and LCA strains were resuspended in 2.5 μM dihydrodichlorfluorescein diacetate (DCFH-DA) (Sigma-Aldrich) in RPMI-1640 in total volume 500 μl and subsequently co-incubated with MH-S cells in a total volume of 100 μl RPMI-1640 medium at MOI = 5. MH-S cells alone were co-incubated in 50 ng/ml phorbolmyristate acetate (PMA; Sigma-Aldrich) as positive control. The fluorescence intensity was measured over a time period of 5 h at 37 °C at 485/535 nm by using a plate reader (TECAN, Infinite M200, PRO). At least three independent biological replicates were performed.

2.9. Galleria mellonella infection model

For virulence tests in the *Galleria* infection model, sixth-instar larvae of *Galleria mellonella* (SAGIP, Italy) were used. Larvae were stored in the dark at 18 °C prior to use for at least 48 h, but not more than 1 week. Larvae weighing between 0.3 and 0.4 g were selected for the experiments and 10 larvae per sample were placed in a petri dish. Spore inocula were diluted in insect physiological saline (IPS: 8.76 g NaCl, 0.35 g KCl, 15.76 g Tris-HCl, 3.72 g EDTA, and 4.72 g Na-citrate dissolved in 1 L of distilled water at pH 6.9) and a volume of 20 μl was injected into the hemocoel *via* the hind pro-leg to a final inoculum of 10^7 spores per larva. For each experiment, 20–30 larvae were used. Untouched larvae and larvae injected with 20 μl of IPS served as control. Larvae were incubated at 30 °C or 37 °C, respectively, in the dark and the larval viability was monitored daily up to 6 days. Assays were repeated at least three times, leading to a total of 60 infected larvae per sample. Survival data were evaluated by using Kaplan-Meier survival curves [15] representing the average survival gained from all replicates. Statistical analysis was carried out utilizing GraphPad PRISM statistics software ver. 6.0. Significant difference was defined by a p-value of <0.05.

2.10. Spore surface ultrastructure by Atomic Force Microscopy (AFM)

Resting and treated spores of LCV and LCA strains of *L. corymbifera* were fixed in 4.0% (v/v) formaldehyde (Serva, 31628) in PBS for 10 min, then the washing step was repeated three times with PBS 10 μl of spore suspensions were dropped cast on a pre-cleaned cover slip. After drying the sample, topography was investigated with a Nanowizard I AFM (Bruker Nano-JPK BioAFM, Berlin). BudgetSensors Tap190Al-G tips were used to scan the samples in intermittent contact mode with a resolution of 256 × 256 px as described previously [24,25].

2.11. Episporic ultrastructure by Transmission Electron Microscopy (TEM)

Freshly harvested resting and treated spores were collected by centrifugation at 6300*g* for 3 min. Small pellets of spores were fixed with 2.5% (v/v) glutaraldehyde (Serva, 23114) in 0.1 M sodium cacodylate buffer (Serva, 15540, pH 7.4) for 24 h at room temperature. After washing 3 times for 15 min each with 0.1 M sodium cacodylate buffer (pH 7.4), the spores were post-fixed with 2.0% (w/v) osmium tetroxide for 1 h at room temperature. During the following dehydration in ascending ethanol series post-staining with 1% (w/v) uranylacetate was performed. Afterwards the samples were embedded in epoxy resin (Araldite) and sectioned using a Leica Ultracut S (Leica, Wetzlar, Germany). Finally, ultrathin sections were mounted on filmed Cu grids, post-stained

with lead citrate, and studied in a transmission electron microscope (EM 900, Zeiss, Oberkochen, Germany) at 80 kV and magnifications of 3000x to 50,000x.

2.12. Luciferase reporter activation after stimulation of Toll-like receptor-expressing (TLR) Flp-In™-293 NF-κB cells with spores of Lichtheimia corymbifera

2.12.1. Toll-like receptor and cofactor coding plasmids

Plasmids coding for Toll-like receptors (TLR) were purchased from Addgene (www.addgene.org): pcDNA3-TLR1-YFP, pcDNA3-TLR2-YFP, pcDNA3-TLR4-YFP, pcDNA3-TLR5-CFP, pcDNA3-TLR6-YFP, pcDNA3-CD14 (Addgene plasmids # 13014, # 13016, # 13018, # 13019, # 13020, # 13645) were a gift from Douglas T. Golenbock (University of Massachusetts Medical School, division of Infectious Disease and Immunology, Worcester, MA, USA) to Addgene).

2.12.2. Cloning of TLR combinations into pcDNA5/FRT or pEXPpRRLR4R3-Neo

Combinations of TLRs were cloned into pcDNA5/FRT (Invitrogen, Thermo Fisher Scientific, Waltham, USA) or pEXPpRRLR4R3-Neo backbone that was derived from pEXPpRRLR4R3-Neo-p65 vector. This p65 containing vector was a kind gift of Alexander Loewer (Technical University of Darmstadt, Systems Biology of the Stress Response, Darmstadt, Germany), published with a p53-insert [26]. The p65-insert was replaced by inserts encoding Toll-like receptors and essential cofactors. This vector is based on the pRRL vector that was published before [27]. For cell line generation the following TLR combinations were cloned in one open reading frame by linking with T2A sequences under control of the CMV promotor: TLR2_TLR1_CD14, TLR2_TLR6_CD14, TLR2_CD14, TLR5 and TLR4_MD2_CD14. Toll-like receptors and cofactors CD14 and MD2 were cloned into one open reading frame linked by T2A sequences.

2.12.3. Cloning of the NF-κB responsive promoter

A promotor construct of 220 bp was synthesized containing three different binding motifs for the p65 and p50 subunit of NF-κB (5́-GGGGACTTTCC-3́,5́-GGGGATTCCC-3́, 5́-GGGGATTTCC-3́) flanked by restriction enzyme sites for EcoNI (5́) and HindIII (3́) 12,13. An additional NF-κB response element and a TATA-like sequence from pNFκB-Luc vector (Clontech, 631904) were added to the Firefly luciferase gene and introduced into pCDH-CMV-EF1-Puro.

2.12.4. TLR5 knock out with CRISPR/Cas9

For Cas9-induced TLR5 knock out, the online guide design tool www.crispr.mit.edu was used to design the following oligo: TLR5-guide-forward CCGGACCACCTGGACCTTCTCCT and TLR5-guide reverse AAACAGGAGAAGGTCCAGGTGGTC (Nucleotides in bolt represent overhangs for cloning). Both guides were cloned into pGuide-it-tdTomato (TaKaRa Bio Europe) according to the manufactureŕs protocol.

1.5 million HEK-NF-κB luciferase reporter cells and 1.5 million TLR2-CD14 expressing HEK-NF-κB luciferase reporter cells were seeded per well of a six well plate (Greiner Bio-One) in 2 ml DMEM supplemented with 10% FBS and 1% Penicillin/Streptomycin (Pen/Strep 10,000 U/ml) and incubated for 12–16 h in a humidified 5% (v/v) CO_2 incubator at 37 °C. Cells were transfected with 3 μg pGuide-it-tdtomato with inserted TLR5-specific guides and 12 μl Lipofectamine 2000 transfection reagent (Invitrogen) per well. 24 h post transfection cells were washed with DPBS, trypsinized and collected in 1 ml DPBS. Cells positive for red fluorescence were sorted with a BD FACSAria™ Fusion. Single cell deposition into 96-well cell culture plates was performed. Single cells were grown in 300 μl conditionized DMEM supplemented with 10% FBS, 1% Pen/Strep and 10 μM StemMACS Y27632 (Miltenyi). 24 h later medium was changed to DMEM supplemented with 10% FBS and 1% Pen/Strep. Cells were expanded and analyzed for stimulation by Flagellin as described above. Non-responding cells were characterized by amplifiying a product of TLR5 with the following primers: TLR5_forward-2 TGTCTGTATCTGCCAACAGC and TLR5_reverse-2 AAGGAGAGCGTTTTCCCTTGT. The product of 800 bp was sent for sequencing to Eurofins Genomics, Germany.

2.12.5. Cell line generation by lentiviral transduction to obtain an NF-κB responsive Flp-In™-293 luciferase reporter cell line and TLR4-MD2-CD14 expressing NF-κB responsive Flp-In™-293 luciferase reporter cell line

1.4×10^6 HEK293T cells were seeded in 3 ml Dulbecco's modified eagle medium (DMEM, Thermo Fisher Scientific, Waltham, USA) with 10% fetal calf serum (FCS, Merck Biochrom, Berlin, Germany) into cell culture dishes (diameter 60 mm) and incubated overnight in a humidified incubator at 37 °C at 5% (v/v) CO_2. For viroid production cells were transfected with 2 μg of pCDH-CMV-EF1-Puro, containing the NF-κB responsive promoter and the Firefly luciferase, and 3.4 μg of the packaging plasmids pMDLg/pRRE (Addgene, #12251), pRSV-Rev (Addgene, 12253) and pMD2.G (Addgene, 12259). Plasmids were diluted in 150 μl 0.25 M of $CaCl_2$ and mixed with 150 μl 2x BES (50 mM BES, 280 mM NaCl, 1.5 mM Na_2HPO_4. 2 H_2O, pH 6.95). After 10 min of incubation at room temperature the transfection mix was added dropwise to the cells. After 16 h of incubation at 37 °C at 5% (v/v) CO_2, the supernatant was removed and cells were washed twice with DMEM and another 3 ml fresh DMEM with 10% (v/v) FCS was added. 48, 72, and 96 h post transfection supernatant was collected, sterile filtered and immediately frozen at − 80 °C. Flp-In™-293 cells (Thermo Fisher Scientific) were seeded into 24-Well plates with 5×10^4 cells/well in 0.5 ml DMEM with 10% (v/v) FCS. Cells were incubated overnight and treated three times (0 h, 6 h, and 18) hours with 500 μl of viroid containing supernatant. 6 h after the last infection step medium was changed to DMEM containing 10% (v/v) FCS, 1% (v/v) Penicillin/Streptomycin (Pen/Strep 10,000 U/ml) and 1 μg/ml Puromycin (Invivogen, San Diego, USA) for antibiotic selection. Cells were referred to as Flp-In™-293 NF-κB cells.

For generating the TLR4-MD2-CD14 expressing Flp-In™-293 NF-κB cells, HEK293T were transfected with pEXPpRRLR4R3-Neo-CMV_CD14_T2A_MD2_T2A_TLR4 according to the protocol above. Viroid-containing supernatant was collected to infect Flp-In™-293 NF-κB cells, which were selected with 150 μg/ml G418 (Merck Biochrom, Berlin, Germany).

2.12.6. Stable integration of TLRs by Flp-In™-System

5×10^6 Flp-In™-293 NF-κB cells were seeded into T75 cell culture flask in 10 ml containing 10% (v/v) FCS and incubated in a humidified incubator at 37 °C under 5% (v/v) CO_2 until cell reached a confluency of about 90%. 2 μg of pcDNA/FRT containing cloned TLR combinations and 18 μg of pOG44 were diluted in 600 μl DMEM. Another 600 μl DMEM with the addition of 40 μl Roti ® -Fect (Carl Roth, Karlsruhe, Germany) was added and the mixture was incubated at room temperature for 20 min and added dropwise to the cells. After 24 h of incubation cells were washed with 10 ml DPBS (Thermo Fisher, A1285601) and 10 ml DMEM containing 10% (v/v) FCS, 1% (v/v) Pen/Strep (10,000 U/ml) was added. 48 h after transfection cells were splitted 1:4 and 300 μg/ml Hygromycin (Thermo Fisher, 10687010) was added to the cell culture medium for antibiotic selection of stably transfected cells. After 24 h, the medium was changed to DMEM (Thermo Fisher, 12491015) with 100 μg/ml Hygromycin and incubation was continued until

cell foci appeared. Cell lines were referred to as Flp-In™-293 NF-κB _TLR cells.

2.12.7. TLR activation-induced luciferase assay

5×10^4 Flp-In™-293 NF-κB -TLR cells were seeded per well of a 96-well plate (Greiner Bio-one, Frickenhausen, Germany) in 145 μl DMEM containing 4.5 g/l glucose, 10% (v/v) FCS, 1% (v/v) Pen/Strep, 1 mM L-Glutamin, and 250 μM Luziferin D (Promega, Madison, USA). Cells were incubated 12–16 h in a humidified incubator at 37 °C under 5% (v/v) CO_2 to adhere to the bottom of the plate. The plate was sealed prior to the measurement in a TopCount®NXT (PerkinElmer, Waltham, USA) microplate luminescence counter at 37 °C. The cells were run without stimulation for 2 h (pre-run) and stimulated afterwards by fungal spores. Spores of *L. corymbifera* strains LCA and LCV were added to a final concentration of 1.6×10^6 spores/ml and were pre-treated the following way: (a) heat-killed, (b) kitalase treatment, (c) kitalase treatment followed by heat-killed, (d) heat-killed followed by kitalase treatment, (e) Pronase E treatment, (f) heat-killed and Pronase E treated, (g) UV-treated, (h) Vinotaste-treated, and (i) heat-killed and Vinotaste treated. Resting spores were used as control as well as unstimulated cells where medium was added instead of spores. Luminescence measurement continued for additional 16 to 20 h at 37 °C. Luciferase values were normalized by the mean of the pre run values of each well.

3. Results

3.1. The determination of the optimal parameters for in vitro phagocytosis assay

In order to monitor the phagocytosis index (PI) of resting spores of *L. corymbifera* by macrophages, spores were coincubated with macrophage cells for various time points (1, 3, and 5) hours to determine the difference between LCV and LCA strains using a MOI of 5 as defined by 5 spores per 1 macrophage (Fig. 1A). The highest phagocytosis index was achieved at the time point of 3 h of confrontation of macrophages with the spores of LCA, whereas the PI is still slightly increasing beyond 3 h of confrontation with LCV.Then swelling and opsonization with normal human and mouse serum were tested in this experimental setting for *in vitro* phagocytosis (Fig. 1B). Swelling of the spores did not affect the PI whereas opsonization process increased significantly the PI normalized to the resting spore conditions to almost equal extents in both strains. This observation works for human and murine serum, and hence is independent of the origin of mammalian serum (Supplementary Fig. 1). In general, the strongest effect of opsonization on PI was confirmed at the 3 h' time point of confrontation, even though the PI of opsonized spores of LCV and LCA was similar to resting spores after coincubation for 5 h (Supplementary Fig. 2). The reduced phagocytosis after opsonisation of LCA can be explained by the strongly reduced phagocytosis of swollen LCA spores which in addition germinated faster than the spores of LCV (Supplementary Fig. 3). The kinetics of swelling and germination is linked to phagocytosis and appears to be epispore-dependent.

3.2. Spore surface modifications of L. corymbifera increased the rate of phagocytosis by MH-S cells

In order to shed light on the contribution of the fungal epispore, the individual outer spore surfaces were treated or shaved layer by layer using physical or chemical treatments as described in details in the methods part of the spores of the virulent strain compared to the attenuated strain of *L. corymbifera* (LCV *vs* LCA, respectively)

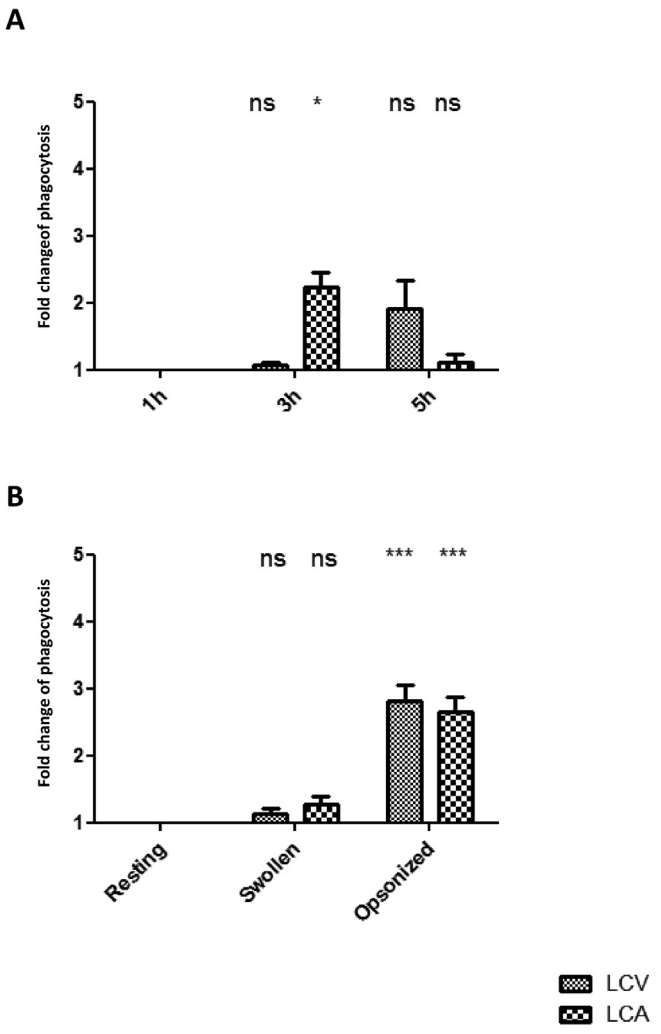

Fig. 1. phagocytosis the spores of *L. corymbifera* by alveolar macrophages (MH-S). A) Comparative phagocytosis assay between two *L. corymbifera* strains: *L. corymbifera* virulent strain (LCV) and *L. corymbifera* attenuated strain (LCA) in a time-dependent interaction with murine alveolar macrophages at MOI of 5 as indicated by fold change phagocytosis index normalized to the minimal time point of 1 h. The statistical analysis using *t*-test applies the 1 h time point as reference for comparison with 3 h and 5 h time points. B) Phagocytosis after swelling and opsonization with normal human serum in comparison to resting spores of two *L. corymbifera* strains: *L. corymbifera* virulent strain LCV and *L. corymbifera* attenuated strain LCA confronted with murine alveolar macrophages for 3 h as indicated by fold change phagocytosis index normalized to the resting spore condition. The statistical analysis using *t*-test applies the resting spore condition as reference for comparison with swollen and opsonized spores. ns. . .non-significant, * $P < 0.05$, ** $P < 0.01$, *** $P < 0.001$.

(Fig. 2). The effect of spore treatments was determined in comparison to untreated living and heat-killed resting spore conditions for negative and positive control, respectively (Fig. 2). In general, treatment of the spores with Tween 20 has the smallest influence on PI, which is not significantly different $p > 0.05$, whereas shaving of the spores with Pronase E expresses the highest influence on the PI of both strains (Fig. 2). When both strains were compared, LCA was more affected by spore surface modification than LCV as indicated by 1.5 – 3.8 and 1.0 – 2.5 fold change increase of PI for the attenuated *vs* the virulent strain, respectively (Fig. 2). Glucanolytic treatment by kitalase (β-1, 3-glucanase) and Vinotaste (crude extract of glucanases, proteases and pectinases used for baker's yeast in wine maturation) enhanced the PI compared to the resting spore conditions (Fig. 2). In LCA, the PI was even more pronounced when spores were treated with kitalase (Fig. 2). The biggest influ-

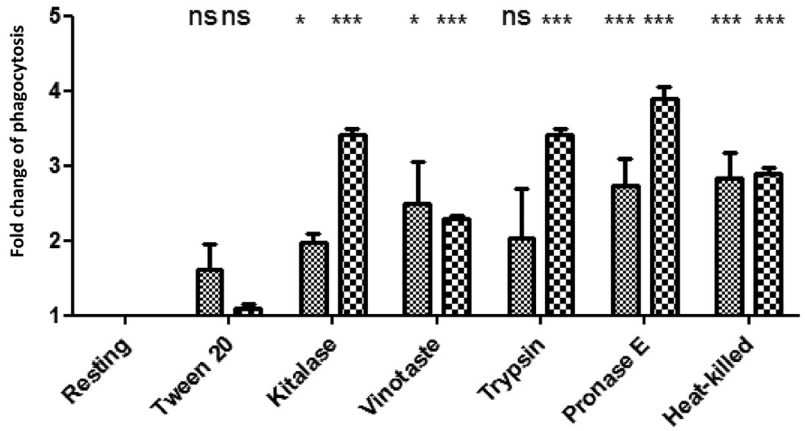

Spore wall component	Modulating influence on the spore wall [+/-]						
Lipids	-	+	-	-	-	-	-
Glucans	-	-	+	+	-	-	-
Proteins	-	-	-	+	+	+	+
Viability	-	-	-	-	-	-	+

Fig. 2. Phagocytosis after physical and enzymatic treatments of spores of two *L. corymbifera* strains: *L. corymbifera* virulent strain (LCV) and *L. corymbifera* attenuated strain (LCA) in interaction with murine alveolar macrophages for 3 h (MOI = 5) as indicated by phagocytic indices normalized to resting spores. The table below displays the spore wall components structurally and qualitatively affected during the treatment. + indicates, affected', - indicates, not affected'. The statistical analysis using *t*-test applies the resting spore condition as reference for comparison with the other spore treatments: ns non-significant, * $P < 0.05$, ** $P < 0.01$, and *** $P < 0.001$.

ence of enzymatic modification of resting spores was achieved with proteo-glucanolytic treatments using kitalase, trypsin (an endopeptidase and serinprotease which selectively digests lysine, arginine and modified cysteine peptide bonds), and pronase E (a crude preparation of proteolytic enzymes obtained from *Streptomyces griseus*) (Fig. 2). This increase on PI was quantitatively comparable to the PI of opsonized spores (Supplementary Fig. 1). Treating the spores with trypsin increased the PI value for both strains (LCV and LCA); however it is statistical significant difference for the LCA strain not the LCV stain (Fig. 2). In general, the PI was highly increased a result of spore treatments for both strains; meanwhile the PIs of LCA was less prone to high standard deviations. In order to prevent side effects of spore germination preceding confrontation with the macrophages, the spores were subjected to germination kinetic assays after spore treatments (Supplementary Fig. 3). None of the treated spores were germinated after 3 h, the time point used for confrontation during phagocytosis by MH-S. Whereas spore germination of LCV was not affected at none of the time points measured (Supplementary Fig. 3A), the spores of LCA revealed a differential germination pattern as shown in supplementary (Supplementary Fig. 3B). After 5 h, the spore conditions reached a maximum in differential germination: tryptic shaving increased and pronase E digest decreased germination of spores in the attenuated strain (Supplementary Fig. 3).

While the germination analysis focused on the formation of the germination tube, the effect of the treatments may become obvious also during cell swelling. Therefore, we performed a time-lapse analysis of spore germination taking also the spores swelling into account. Assisted by the ImageJ plugin HyphaTracker [19]. We analyzed the spore/germling area over time of LCV and LCA spores after the various treatments by means of video microscopy (Fig. 3). Our analysis revealed that there are no differences between the untreated spores of LCA and LCV strains regarding the germination dynamics (Fig. 3 A, B). Also the treatment with cell wall lytic enzymes let none or only very weak change in the growth behavior of both strains (Fig. 3 C). Using a lag-time exponential model to interpret fungal growth [18,19]. We defined the mean parameters and standard deviation for offset (initial area) and growth rate constant *k*. (Table 1). For LCA, there was not significant effect of the cell wall treatment on the initial area size with exception of trypsin, where LCA showed increased offset parameters (Table 1, Fig. 3C). In contrast, for LCV, the initial increase in the area size was

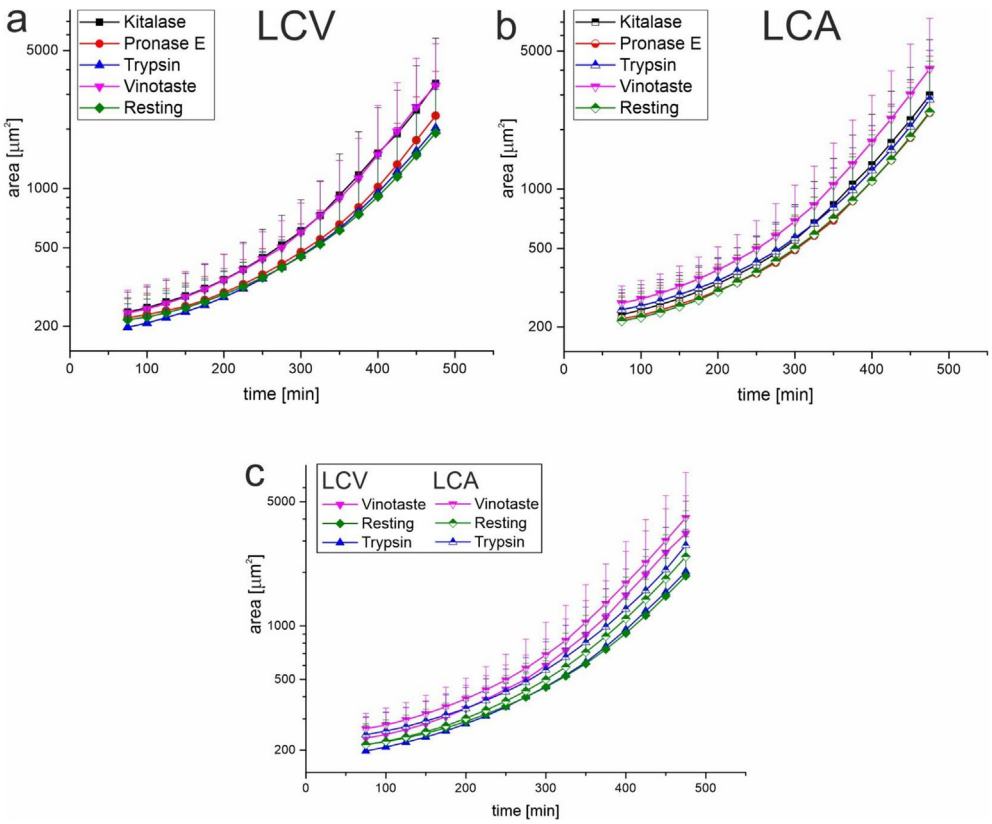

Fig. 3. Time lapse analysis of spore germination of *L. corymbifera* strains (LCA and LCV) after different cell wall treatments. Germination was documented by video microscopy and analyzed with the ImageJ plugin HyphaTracker. The area of each spore/germling was determined at each time points. A,B. Mean values and standard deviation of spore/germling area *vs* time of resting spores or spores treated with kitalase, pronase, trypsin or vinotaste as indicated. C. Parameters obtained by fitting the experimental data with a lag-exponential model showing offset.. Significance values are given in Table 1.

observed after treatment with Kitalase and Vinotaste (Table 1, Fig. 3C). In both cases, the growth rate was significantly increased. The latter was also increased after treatment with Pronase E. In contrast for trypsin treated germlings the initial area of LCV spores was decreased, but the rate was not significantly changed (Table 1, Fig. 3).

When the treatments were compared between both strains, we found significant differences for initial area after treatment with trypsin, with increased areas for the LCA strain (Table 1, Fig. 3C). In terms of the growth rate, the treatment with kitalase and pronase E led to a significant increase in growth rate of LCV in comparison with LCA (Table 1, Fig. 3).

Table 1
Mean values and standard deviation for offset and growth rate after spore treatment with five cell wall-lytic enzymes. *P* values of two-group student's *t*-test are indicated for comparison with either resting spores or for comparison between LCV and LCA strains.

Treatment	Offset VS	SD VS	Offset AS	SD AS	*p* (comparison to Resting)	*p* (comparison VS/AS)
Resting	216.9	70.7	–	–	–	0.93764
–	–	–	217.3	78.8	–	0.93764
Kitalase	242.8	80.4	–	–	**0.0082**	0.19052
–	–	–	226.6	71.0	0.33748	0.19052
Pronase E	229.3	74.8	–	–	0.16311	0.48261
–	–	–	221.0	77.7	0.69757	0.48261
Trypsin	199.2	71.9	–	–	**0.01296**	**1.36E−07**
–	–	–	256.4	91.3	**7.11E−05**	**1.36E−07**
Vinotaste	237.3	74.5	–	–	**0.04314**	0.05881
	–	–	261.9	68.0	**2.68E−05**	0.05881
Treatment	**Growth rate VS**	**SD VS**	**Growth rate AS**	**SD AS**	**p (comparison to Resting)**	**p (comparison VS/AS)**
Resting	0.01073	0.00219	–		–	0.33482
–	–	–	0.01092	0.00297	–	0.33482
Kitalase	0.01197	0.00209	–	–	**3.87E−06**	**2.89E−04**
–	–	–	0.01012	0.00358	0.0891	**2.89E−04**
Pronase E	0.01182	0.00209	–	–	**2.70E−05**	**8.79E−04**
–	–	–	0.0104	0.00321	0.18395	**8.79E−04**
Trypsin	0.0105	0.00244	–	–	0.33943	0.18411
–	–	–	0.01099	0.00317	0.83615	0.18411
Vinotaste	0.01206	0.00177	–	–	**4.40E−07**	0.93067
			0.01214	0.00603	0.14325	0.93067

3.3. Spore surface modification of L. corymbifera has differential influence on intracellular acidification in phagocytes

The result showed that resting spores of LCV and LCA strains inhibited the acidification mechanism of macrophages. None of the enzymatic treatments (kitalase, vinotaste, and pronase E) had a clear effect on the acidifcation of the spores confronted with MH-S cells for 3 h compared to untreated spores and heat-killed spores used as negative and positive controls of phagolysomal fusion-mediated spore acidification, respectively (Fig. 4A). Because of the observed delay in spore germination, trypsinization was performed for phagocytosis kinetics measurements using spores of both strains (Fig. 4B). After 8 h of comparison, the rate of acidification reached a maximum, which was more pronounced in LCA during treating the spores with trypsin. Chloroquine, which is known to have a differential influence [28,29] on phagolysosomal fusion reduced the acidification in the resting spore condition of LCV strain and has no preventive effect for phagolysosomal fusion in the heat-killed spore condition of LCV strain (Fig. 4C). The temporal kinetics of phagolysosomal fusion in a single cell analysis of human monocytes during interaction with the resting and treated LCV and LCA spores were monitored using HIS and revealed that the apoptotic monocytes cells remained acidic throughout the time frame whereas the healthy ones were acidified in the beginning. It could be that the cells are in different stages of apoptosis. However, the cells recovered from the acidification after few hours (Supplementary Fig. 4). In comparison with the apoptotic monocytes *vs* non-apoptotic monocytes infected with resting (not treated spores) and the heat inactivated spores, the cells phagocytosed the spores and acidified within 3 h of confrontation in both the cases. However, there was a second drop in pH in virulent strain after 6 h post infection. Then the cells recovered from the acidic pH to neutral in *L. corymbifera*, LCV and LCA strains gradually (Supplementary Fig. 4). It could be that according to pervious study [17], the excessive acidification of the cell caused by mitochondrial disintegration can still be can be recovered with the presence of pigmented spores. Germination of spores was observed within the monocytes with resting spores after few hours. Therefore, multiple cells were analyzed with HSI after comparison with spores upon different enzymatic treatments in comparison to resting, swollen, and heat-killed spore conditions (Supplementary Fig. 5) as follows: the treatment with pronase E and vinotaste showed highest acidification of the monocytes in both the apoptotic *vs* non apoptotic cells. Though, the cells are recovered after 15 h post infection to neutral pH. The initial acidification demonstrates that pronase E treated spores and the vinotaste spores triggered the phagolysosome formation faster than the other treatments assumable leads to spore death or change in their virulent pattern. In particular, the apoptotic cells seems to have gradual recovery from the acidic pH to neutral (Supplementary Fig. 5). Swollen spores, Trypsinized spores, and Tween 20- treated spores are highly distinct in their influence on the acidification pattern of monocytes as well as the monocytes recovery in comparison with the other treatments. The pattern demonstrates that the monocytes were highly acidic from 0 h post infection until the end of the measurement 48 h. It might indicate that the spores are being trapped and cannot prohibit the monocytes acidification (Supplementary Fig. 5). Collectively, the monocytes always recovered from apoptosis regardless which treatment was used. This effect was more pronounced in apoptotic then in non-apoptotic cells.

3.4. Spores of L. corymbifera inhibit the apoptosis of macrophages

The capability of three different episporic states to inhibit apoptosis was evaluated in murine alveolar macrophages (MH-S). The resting, heat-killed, and UV-killed spores of LCV and LCA strains

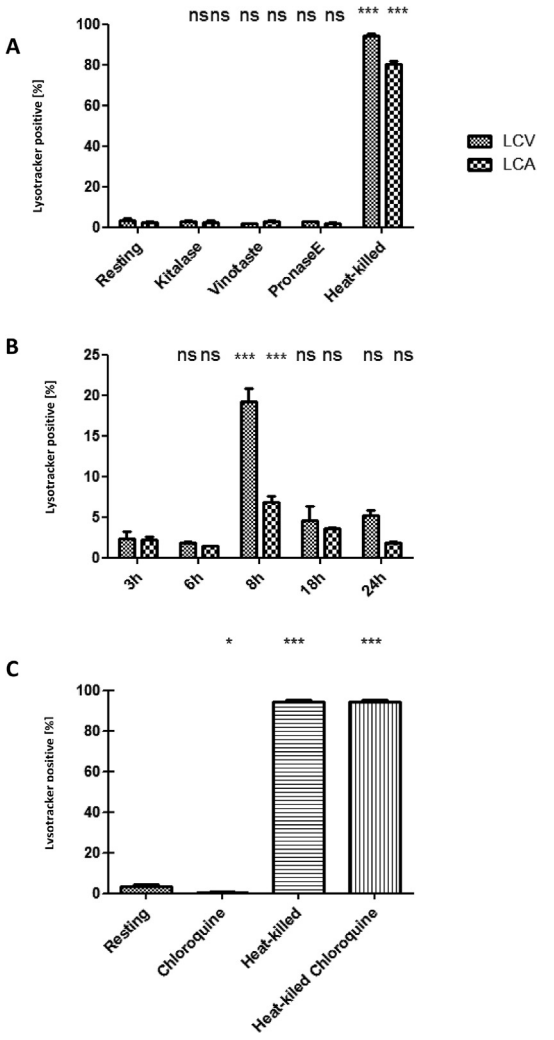

Fig. 4. Phagolysosomal acidification of spores of *L. corymbifera* strains (LCV and LCA) during interaction with murine alveolar macrophages (MOI = 5). (A) Phagolysosomal acidification during the phagocytosis of kitalase, vinotaste, and pronase E-treated spores at time point 3 h of confrontation with MH-S cells compared to untreated (resting) and heat-killed spores for negative and positive control, respectively, (B) Temporal kinetics of phagolysosomal acidification after tryptic treatment, (C) Influence of chloroquine on phagolysosomal acidification triggered by resting *versus* heat-killed spores for LCV spores. Relative acidification was determined by counting the number of acidified phagocytosed spores in relation to 100 phagocytosed spores. Significance values were conducted with *t*-test: ns non-significant, * $P < 0.05$, ** $P < 0.01$, and *** $P < 0.001$.

were able to inhibit the apoptosis of MH-S cells compared to macrophages treated with staurosporine used as positive control (Fig. 5) (Supplementary Fig. 6A-B). Measuring the early, the late, and the whole apoptosis processes revealed that resting, heat-killed, and UV-killed spores of LCV and LCA strains inhibited the whole apoptosis process; however the statistical analysis showed that the resting spores of LCV strain did not affect the value of early and late apoptosis processes compared to MH-S cells incubated with staurosporine (Fig. 5A-C). Moreover, the rate of necrosis was not changed except during incubation with UV-killed spores of LCA strain that was slightly increased and statistically significant difference compared to incubation MH-S cells with staurosporine (Fig. 5D). Heat-killing was performed to be representative for loss of viability and protein degradation, whilst UV-killing was carried out to be representative for loss of viability by parallel maintenance of the outer protein layer. This inhibition was universal for resting spores, heat-killed and UV-killed spores of both strains,

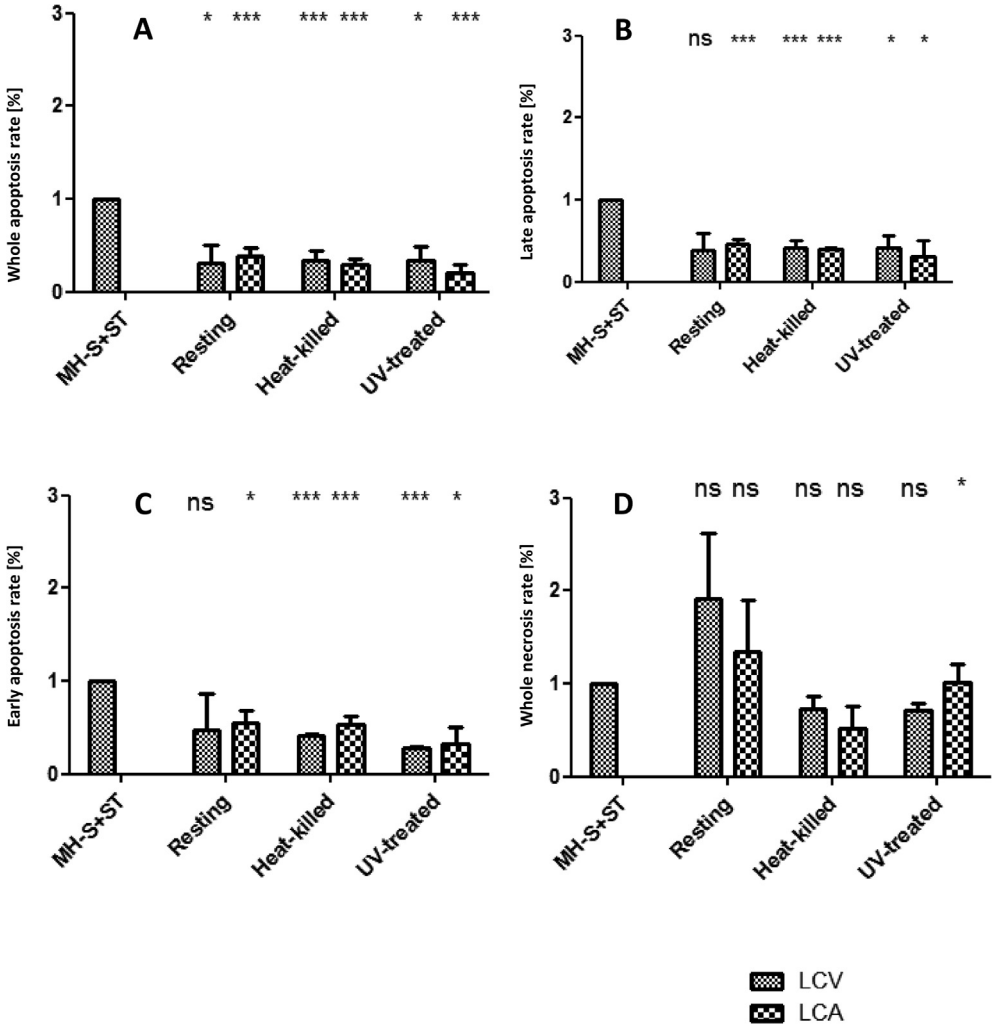

Fig. 5. Induction of apoptosis by *Lichtehimia corymbifera* after physical treatments of spores in murine alveolar macrophages (MH-S). Resting spores, heat-killed spores, and UV-treated spores of LCV and LCA strains of *L. corymbifera* were compared to MH-S cells treated with staurosporine for positive control for the induction of apoptosis in MH-S. The measures represent additive values of the apoptotic stages (early and late apoptosis, and necrosis). (A) The whole apoptotic rate of MH-S cells (early and late apoptosis process), (B) the rate of late apoptotic of MH-S cells, (C) the rate of early apoptosis process of MH-S cells, (D) The rate of necrotic MH-S cells. Three independent biological measurements were performed by Flow Cytometry. Charts of flow cytometry of 1st replicate are shown in Supplementary Fig. 5 as an example. The statistical analysis was based on the percentages of apoptotic and necrotic MH-S cells co-incubated with resting, heat-killed, and UV-treated spores to MH-S cells and compared to MH-S cells treated with staurosporine as positive control. The statistical analysis using *t*-test applies this positive control as reference for comparison with swollen and opsonized spores: ns... non-significant, * $P < 0.05$, ** $P < 0.01$, and *** $P < 0.001$.

which suggests the contribution of the glucan matrix of the spore surface in the inhibition of apoptosis. The effect of UV was significantly higher suggesting a more pronounced role of the protein corona to apoptosis inhibition (Fig. 5), (Supplementary Fig. 6).

3.5. *L. corymbifera* spores increase reactive oxygen species (ROS) generation in macrophages

For ROS generation, the resting spores of LCA strain increased the ROS production by macrophages, although there is no statistical difference over the whole time points. However, the resting spores of LCV strain increased the ROS production by MH-S cells and statistically significant difference was clear over the whole time points (1, 3, and 5 h) in particular 5 h compared to macrophages alone as control (Fig. 6). Moreover, co-incubating the heat-killed and UV-killed spores of LCV and LCA strains with macrophages increased the ROS production by macrophages; however there is no statistical difference compared to control over the whole time points (Fig. 6). These findings confirmed that macrophages have differential response during interacting with the spores of LCV and LCA strains (Fig. 6).

3.6. Spore surface modifications increase virulence of *L. corymbifera* in *G. mellonella*

In order to monitor the impact of various spore treatments on their virulence potential, an invertebrate model was used. In general, LCA was less virulent than LCV in the animal model, when compared to IPS and heat-killed spore conditions for negative controls. In LCV, UV treatment showed the highest effect on the attenuation in the wax moth larvae (Fig. 7A, C), meanwhile treatment with Tween 20 expresses the highest survival of LCA (Fig. 7B, D). Besides UV treatment, swelling, treatment of spores with Vinotaste and trypsin, and to a lesser extent treatment with Tween 20 revealed attenuation in virulence potential of LCV (Supplementary Fig. 7). Besides treatment with Tween 20, swelling, and treatment with Vinotaste revealed attenuation of LCA (Supplementary Fig. 8). Trypsinization and β-1,3-glucanolytic treatment with kitalase increased the virulence of LCA by acceleration of the mortality sim-

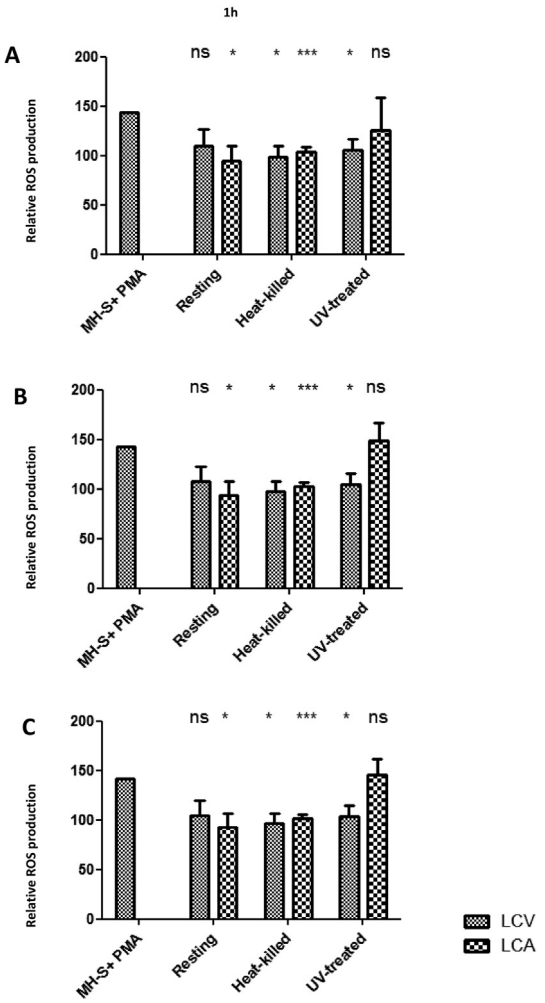

Fig. 6. Generation of reactive oxygen species (ROS) after 1 h (A), 3 h (B), and 5 h (C) of incubation of MH-S macrophages with *L. corymbifera*. Resting spores, heat-killed spores, and UV-treated spores of LCV and LCA strains of *L. corymbifera* were compared to MH-S cells treated with PMA as positive control. The statistical analysis was based on the percentages of ROS production by MH-S cells co-incubated with resting, heat-killed, and UV-treated spores to MH-S cells and compared to MH-S cells treated with PMA as positive control. The statistical analysis using *t*-test applies this positive control as reference for comparison with swollen and opsonized spores: ns. . .non-significant, * $P < 0.05$, ** $P < 0.01$, *** $P < 0.001$.

ilar to LCV by maintaining the spore germination, which is similar between trypsinized compared to non-trypsinized (25 mM NH_4HCO_3) spores (Supplementary Fig. 3). Thus, trypsinization of the spore surface shaves the outer layer of surface proteins towards exposure of key ligands which contribute to higher virulence potential.

3.7. Spore surface modifications alter spore surface ultrastructure of L. corymbifera

In order to display the spore ultrastructural changes after physical and enzymatic treatments, the spore conditions with the highest effect on phagocytosis (Fig. 2) were investigated with AFM (Fig. 8). These were resting spores (Fig. 8A), kitalase-treated spores (Fig. 8B), Vinotaste-treated spores (Fig. 8C), trypsin-treated spores (Fig. 8D), Pronase E-treated spores (Fig. 8E) and heat-killed spores (Fig. 8F) of both strains, LCV and LCA. The topography and amplitude images show an assembly of spores and a more detailed insight into the surface structure of a single spore. In general, the effect of proteolytic treatment was superior to glucanolytic treatment. Proteolytic shaving (Fig. 8D–F) of the spore surface revealed a smoother surface which reached its maximum in the Pronase E treatment (Fig. 8F). The effect of heat-treatment resulted in a flattening of the spores (Fig. 8F) which provided somewhat of a fried egg appearance by maintenance of the roughness as compared to the surface structure of resting spores (Fig. 8A). In order to investigate the impact of episporic modification on spore cross-sections we subjected exemplarily strain LCV to TEM (Fig. 9). The episporic cross-sections were compared to the resting spore conditions and were evaluated in accordance to 3 criteria: (i) cell wall continuity, (ii) relative layer thickness compared to the outer coat and (iii) electron density. More criteria could not be defined in order not to risk conflict with naturally occurring age-dependent spore surface variations. Trypsinization decreased thickness of the outer spore coat relative to the inner layers during incorporation of episporic layers with those of the sub-surface (sub-episporic layers). Pronase E treatment led to fading of the outer spore coat. Heat-killing resulted in coalescence of episporic with sub-episporic layers which was more pronounced than in the trypsinized spore condition (Fig. 9). Electron density in the sub-episporic layer was increased as shown by an increase of granularity. Swollen spore condition is indicated by dilation of the outer and inner spore coats (Fig. 9). A combination of detumescence (subsidence of swelling and fading) of the outer spore coat and increase of the electron density in the sub-episporic layer which is indicative for combined proteolytic and glucanolytic episporic modification performed by Vinotaste treatment (Fig. 9). Delipidation retained spore coat integrity as indicated by the maintenance of cell wall continuity. To sum it up, ultrastructural consequences of episporic modifications could barely visualized by AFM and TEM (Fig. 8 and Fig. 9). Thus, we conclude that the consequences of episporic modifications take place at the level of spore-cell interaction which is addressed by phagocytosis, phagolysosomal fusion and intracellular acidification, apoptosis, generation of reactive oxygen species (ROS), and virulence. In order to address the consequences of episporic modifications at the level of spore-cell communication, the stimulation of Toll-like receptors was monitored as representative for recognition of spores by macrophages (TLRs).

3.8. Stimulation of Toll-like receptors by spores of L. corymbifera after episporic treatments

Toll like receptors (TLRs) belong to the receptor repertoire of the innate immune system and are part of the first line of defense against invading pathogens. They are expressed on a wide range of innate immune cells and recognize a huge amount of viral, fungal and microbial molecules that are named pathogen-associated molecular patterns (PAMPs) [30]. To investigate the ability of *L. corymbifera* spores to activate TLRs, a panel of TLR-expressing cells based on HEK Flp-In™-293 cells was generated. Those cells stably express the following combinations of TLRs and essential cofactors such as CD14 and/or MD-2: TLR2-CD14, TLR2-TLR1-CD14, TLR2-TLR6-CD14, TLR4-MD-2-CD14 and TLR5. HEK Flp-In™-293 cells endogenously express TLR5. To exclude costimulation of TLR5, the gene encoding TLR5 was modified by CRISPR/Cas9 to create a knock-out in the basal cell line and TLR2-CD14 expressing cell lines. Furthermore, the TLR-expressing cells contain a luciferase reporter gene under control of a NF-κB-responsive promotor that indicates signaling from the TLR pathways that result in recruitment of the transcription factor NF-κB. Cells were referred to as TLR- NF-κB luciferase reporter cells. Heat-killed, resting, kitalase treated, kitalase first and heat second treated and *vice versa* treated spores of LCV and LCA were subjected to those cells (Fig. 10). The most remarkable stimulations were achieved in TLR2-CD14 cells, whilst TLR2-TLR1-CD14, TLR2-TLR6-CD14 and TLR4-MD2-CD14

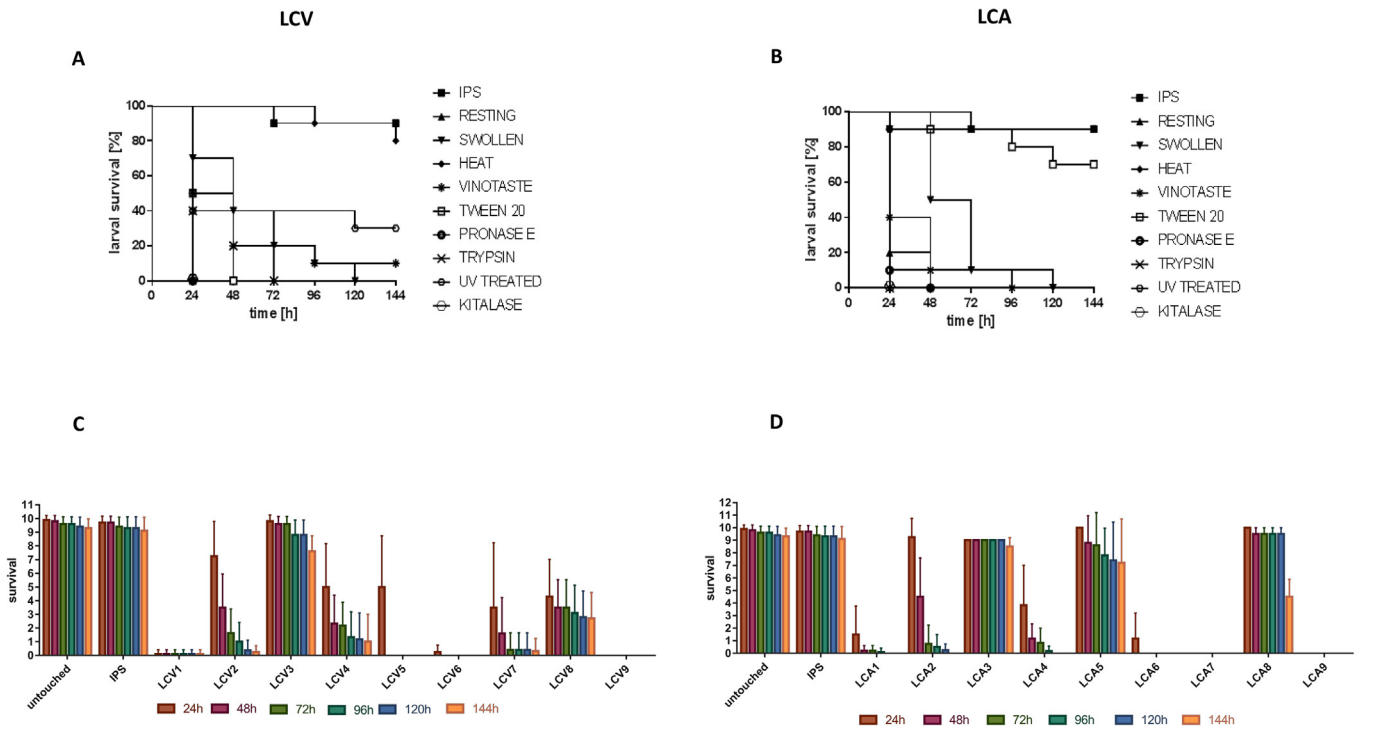

Fig. 7. Virulence of *L. corymbifera* strains LCV (A and C) and LCA (B and D) after physical and enzymatic treatments of spores in *Galleria mellonella*. Larvae were infected with 10^7 spores/larva and incubated at 30 °C in the dark. Survival was monitored every 24 h for six days. (LCV1/LCA1) indicate resting spores of two strains of *L. corymbifera*, (LCV2/LCA2) refer to swollen spores of LCA and LCA strains, (LCV3/LCA3) show the heat-killed spores of LCV and LCA strains, (LCV4/LCA4) refer to the vinotaste-treated spores of LCV and LCA strains, (LCV5/LCA5) show tween 20 treated spores of LCV and LCA strains, (LCV6/LCA6) refer to pronase E-treated spores of LCV and LCA strains, (LCV7/LCA7) show trypsinized spores of LCV and LCA strains, (LCV8/LCA8) show UV-treated spores of LCV and LCA strains, and (LCV9/LCA9) show kitalase-treated spores of LCV and LCA strains. Kaplan-Meier curves represent average survival data of all three independent survival assays and were analyzed for significance by Log-Rank (Mantel Cox) test utilizing graph pad prism software.

cells were stimulated to a lesser extent after confrontation with kitalase treated, kitalase first and heat second treated and *vice versa* treated spores of LCV and LCA whilst TLR stimulation of the cells after exposition to heat-killed and resting spores remained unaffected when compared to the unstimulated control were only medium was added to cells. The spore modifications with kitalase and heat in single and combined treatments revealed significant stimulation of TLR2-CD14 after 10 h of confrontation of TLR2-CD14 expressing Flp-In™-293 NF-κB cells (Fig. 11). TLR2-CD14 expressing NF-κB luciferase reporter cells were chosen to analyze the impact of additional treatment procedures including UV-inactivation, moderately heat-killed treated, Vinotaste-treated, heat-killed first and Vinotaste treated second, Pronase E, heat-killed first and Pronase E second treated spores of LCV and LCA compared to resting, heat-killed treated, kitalase treated, kitalase first and kitalase second treated (Fig. 11). As seen in the first assay with the entire panel of TLR-expressing NF-κB luciferase reporter cells, the strongest stimulation of TLR2 was achieved with kitalase and heat-killed first and kitalase second treated spores of LCV and LCA.

4. Discussion

In advance to this study, two strains of *L. corymbifera* were identified which show differential behavior in virulence and phagocytosis by macrophages and *G. mellonella* as infection models [15,16,31]. The differences were attributed to the spore surface, here named the epispore, of the sporangiospores, here named resting spores. The various structural architecture of the outer surfaces of the pathogenic microorganisms play a central role during interaction with host cells [32–35]. This difference in the phagocytic vulnerability is likely the result of differences in the components of surfaces of the spore cell wall (epispore). Since this increase at time point 5 h is comparable with the PI of LCV at time point 3 h and was not observed for LCA the time point 3 h was defined as the most common denominator and used as standard time for confrontation under MOI of 5 in any follow up phagocytosis assays. The systematic shaving of the epispore layer by layer revealed the contribution of glucans and proteins but to a lesser extent the importance of lipids to the phagocytosis rate by macrophages. Additionally, the carbohydrate structures that are present on the surface of *Lichtheimia* spores manipulated the phagocytosis rate by macrophage cells which speculate that dectin-1 has a role in the recognition as it was shown before its function in the phagocytosis of *A. fumigatus* by murine macrophages [36]. Opsonization of *Lichtheimia* spores of LCV and LCA strains increased the phagocytosis rate by macrophages either through the application of normal human serum or mouse serum and did not change even when the co-incubation time was increased. The current data is concordant with the previous studies that revealed that the spores of Mucorales species such as *Mucor plumbeus*, *M. circinelloides*, *Mucor ramosissimus, Rhizopus arrhizus,* and *Rhizomucor pusillus* could stimulate the human complement system mainly through the alternative pathway and C3 pathway which in turn showed the importance of competent opsonization [37,38]. Moreover, the similarity in the effect of two different sources of serum (human and mouse) on the opsonization process confirmed the importance of the complement system in the recognition of fungal pathogens by immune cells that could be demonstrated before in *A. fumigatus* and *Candida albicans* [39]. This finding shed light on the role of the complement system on the recognition of Mucorales species during invasive infections and their interaction with phagocytes.

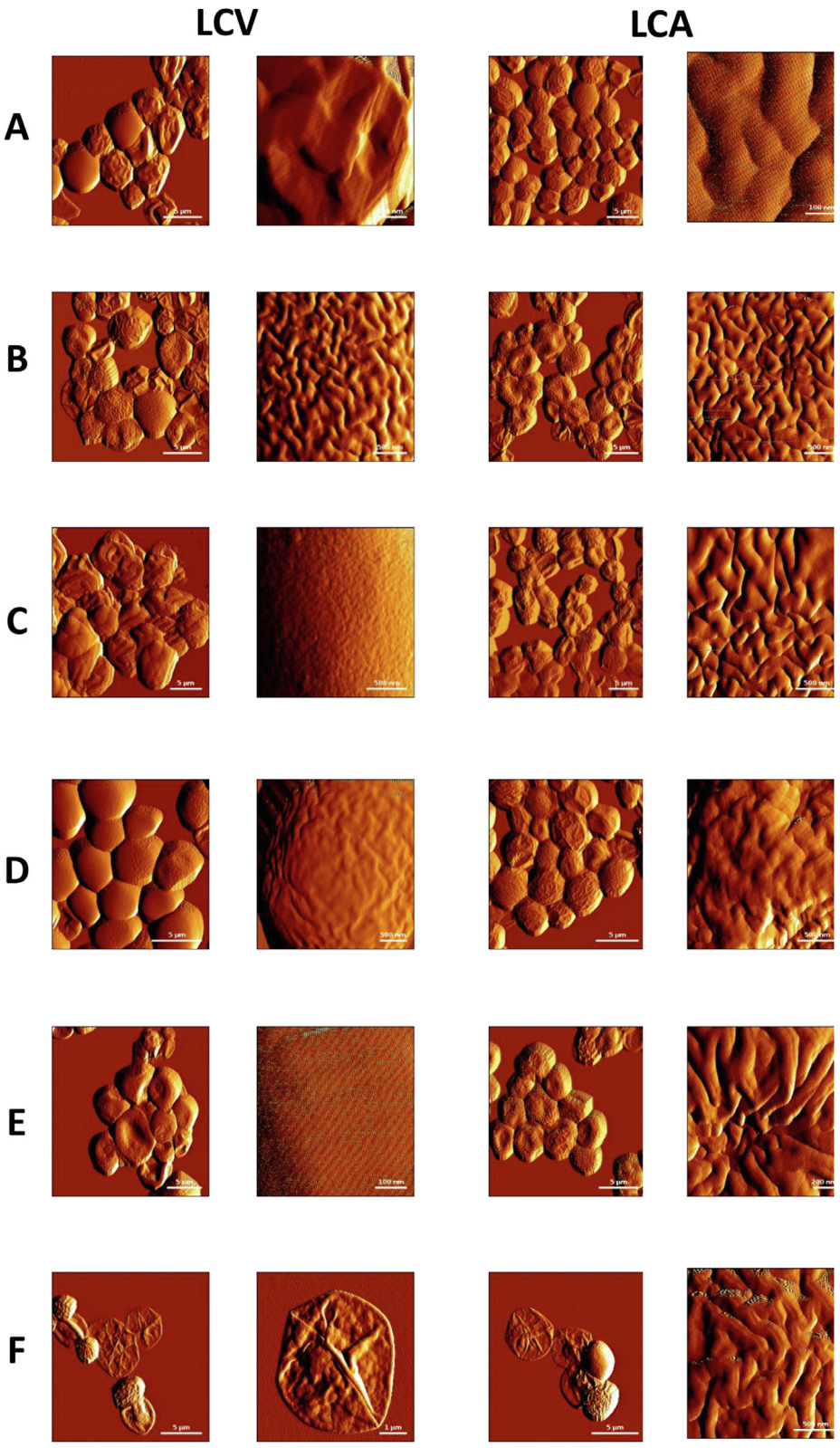

Fig. 8. Topography AFM images show the morphology and ultrastructure of spores of *L. corymbifera* strains (LCV and LCA). A – Resting spores; B – kitalase-treated spores; C – Vinotaste-treated spores; D – trypsin-treated spores, E – Pronase E-treated spores, F – heat-killed spores.

The germination of treated spores did not change from the resting spores which in concordant with previous studies that confirmed that spore surface protein of *Rhizopus delemar* does not influence on the morphological characters of the cells such as germination, growth rate, cell size, and the respiration [2].

Acidification is one an important step in phagosome maturation through decreasing the intra-phagolysosomal pH and subsequent degradation of phagocytosed particles [40]. The inhibition of phagolysosomal fusion monitored by lacking acidification was shown for *A. fumigatus* during interaction with epithelial cells

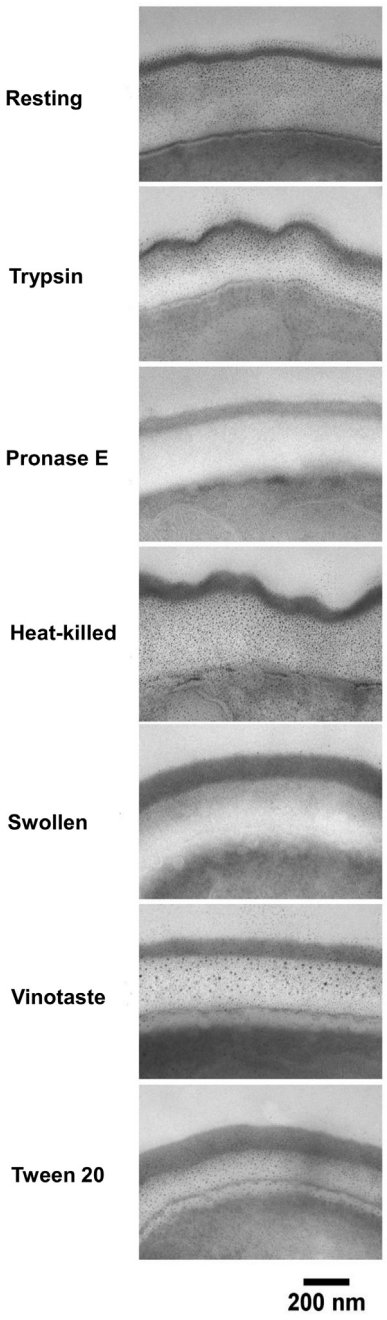

Fig. 9. Ultrastructure of cross-sections from modified epispores of *L. corymbifera* strain LCV performed by Transmission Electron Microscopy (TEM). The cross-sections were taken from sub-sections of the spore surfaces from (i) resting spores and compared to resting spores treated with: (ii) trypsin, (iii) pronase E, (iv) heat, (v) Vinotaste and (vi) Tween 20. The episporic ultrastructures display differences in cell wall integrity as given by (i) cell wall continuity, (ii) cell wall thickness and (iii) electron density. The scale bar indicates 200 nm.

due presence of rely on 1,8-dihydroxynaphthalene (DHN) melanin on the surface of spores [41]. *L. corymbifera* spores lack DHN melanin due to absence of functional genes encoding non-ribosomal peptide synthetases (NRPSs) and polyketide synthases (PKSs) [42,43]. The current study could show that resting spores of *L. corymbifera* LCV and LCA strains inhibited the intracellular acidification of macrophages which is indicative for a novel mechanism to prolong spore survival within macrophage cells independently from DHN melanin. The measurement of the intra-phagolysosomal pH by HSI could answer the question of the role of spore surface structures in the intracellular survival with monocytes as it could prove the role of DHN melanin of *A. fumigatus* in inhibiting the acidification of monocytes [17]. A recent study revealed that the spores of *Rhizopus* species apply eumelanin which is dissimilar in chemical structure to the DHN melanin of *A. fumigatus*, but inhibits phagosome maturation [12], and thus may be important for intracellular survival of Mucorales species during interaction with phagocytes. The present study provides proof for acidification after invagination of trypsinized spores of LCV and LCA strains. This finding confirms the role of spore surface protein candidates in the defense mechanism during interaction with phagocytes which is concordant with the inhibition of phagosomal maturation of macrophages through *STP2* transcription factor that regulates the amino acid transport in *C. albicans* [44]. The determination of the spore surface protein candidate that is responsible for inhibiting the acidification of macrophages is not easy due to difficulties in genetic manipulation of Mucorales species, however CRISPR/Cas9 genome editing method was developed recently for some Mucoromycotina [45,46]. Therefore, the influence of the spore surface protein corona on the inhibition of apoptosis was investigated. Both, spores with and without sustained protein corona inhibit the apoptosis suggesting a major role of the spore and its cell wall matrix as a whole particle in the prevention of apoptosis of the host cell. This sheds light into the nature of *Lichtheimia* spores using macrophages as vehicle for dissemination as discussed before [16] and already described for immune evasion in *Cryptococcus neoformans* [47]. The current study reports the inhibition of apoptosis of macrophages by *L. corymbifera* which is mandatory for protection and survival of *Lichtheimia* spores inside the macrophages over longer time periods. This finding is concordant with the recognition of proteins that inhibit apoptosis of macrophages by *A. fumigatus* but different from *L. corymbifera* by a DHN melanin-dependent mechanism [22,48]. Therefore, the current study raises very promising questions that should be clarified next, e.g. (i) which spore surface proteins are responsible for the reduction of phagolysosomal fusion, (ii) what is the mechanism of apoptosis inhibition, (iii) what are the differences between *A. fumigatus* and *L. corymbifera* with respect to spore architecture and cell–cell communication in consequence of genome evolution and spore pigment composition [49], (iv) what is the host signal pathway of macrophages that contributes in these inhibition processes and (v) if eumelanin is an universal spore component playing a protective role for all Mucorales in intracellular survival as shown exemplarily for *Rhizopus* species [12]. The production of ROS belongs to the inflammatory response that is produced during the interaction with pathogens as part of the immune defense response [50]. The current study revealed that spores of LCV increased the ROS production by macrophages like shown for *A. fumigatus* and *C. albicans* [51]. The receptor Dectin-1 is responsible for the production of ROS by macrophages in response to *A. fumigatus* and *C. albicans* [51]. This finding encourages the role of unknown macrophage receptors in the defense response against Mucorales which were not studied before. The difference in the response of macrophages toward the spores of LCV and LCA strains prompted the assessment of the virulence potential. *G. mellonella* was established as a promising infection model for various species of Mucorales because analogies in read-outs with mammalian models were reported [52]. The current study confirmed the different virulent potential of LCV and LCA strains by conformation of the high virulence of LCV compared to LCA as it was shown before in an avian infection model [15]. Episporic modifications express differential influences on virulence, of which the trypsinization and β-1,3-glucanolytic treatment caused an intriguing increase of virulence indicating a role of spore surface structures during host-pathogen interaction. Ultrastructural analyses by AFM showed that proteolytic treatments make the spore smoother than

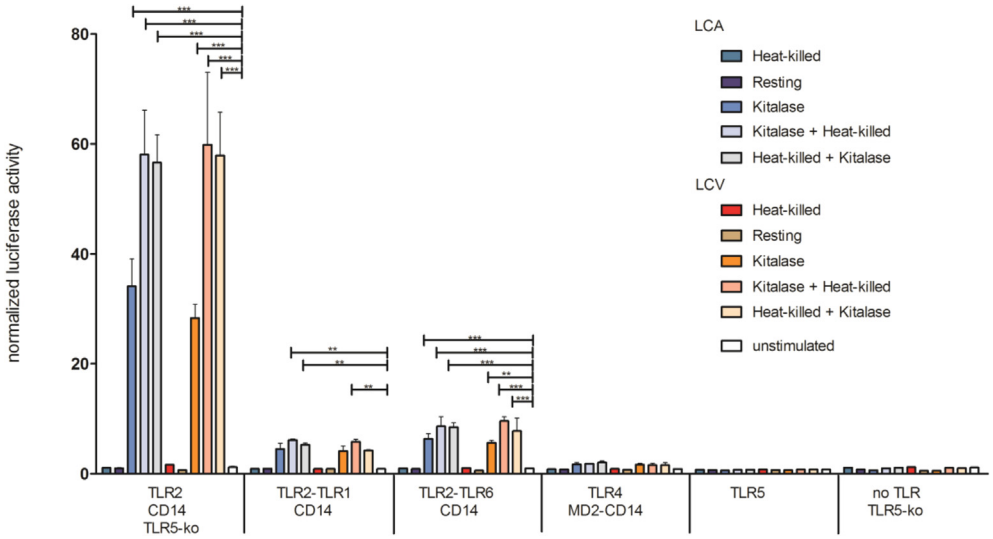

Fig. 10. Luciferase reporter activation after stimulation of Toll-like receptors (TLRs) -expressing Flp-In™-293 NF-κB cells with spores of *Lichtheimia corymbifera* after different treatments for 5 h. Flp-In™-293 NF-κB cells stably expressing different Toll like receptors (TLR1,2,4,5,6) and cofactors (CD14, MD2) and additional knock out of TLR5 (TLR5-ko) were generated for TLR activation assays. All cell lines have a stably integrated promotor that is responding to the transcription factor NF-κB (nuclear factor 'kappa-light-chain-enhancer' of activated B-cells) that translocates from cell plasma to the nucleus upon TLR activation. The responsive promotor regulates the expression of the luciferase reporter gene. The selected TLR combinations were: TLR2-CD14 with TLR5-ko, TLR2-TLR6-CD14, TLR2-TLR1 -CD14, CD14- MD2- TLR4 and TLR5. The basic cell line with luciferase reporter gene was used as comparison and has an additional TLR5-ko of the natural gene. Cell lines were seeded into 96-well-plates. The activity of the luciferase after 5 h of stimulation was normalized to the mean value of the pre run (2 h before stimulation). Data was analyzed by two-way ANOVA and Bonferroni posttest (*** indicates $P < 0.001$, * indicates $P < 0.05$).

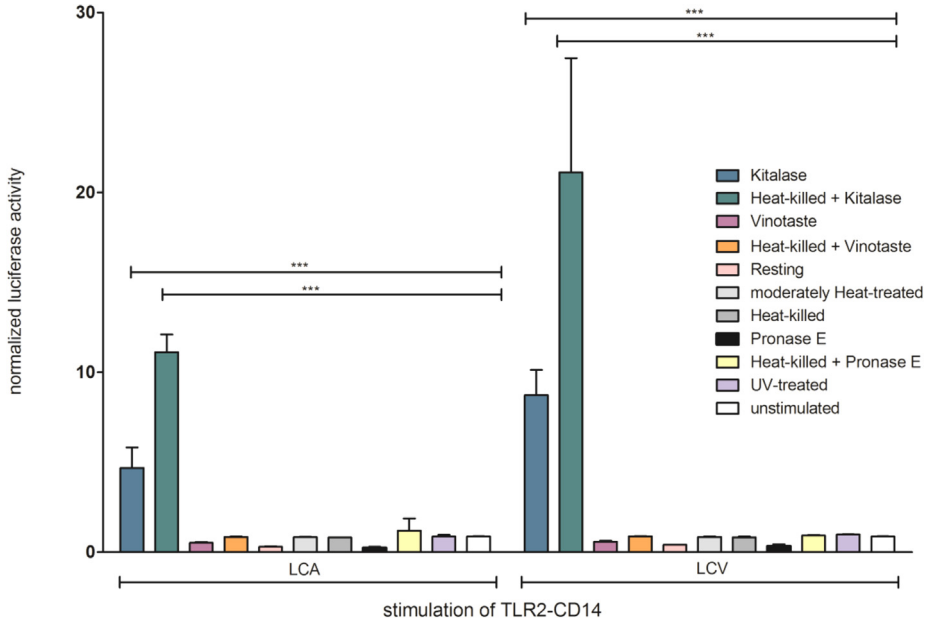

Fig. 11. Luciferase reporter activation after stimulation of TLR 2-CD14 expressing Flp-In™-293 NF-κB cells with spores of *Lichtheimia corymbifera* after different treatments for 10 h. The capability of kitalase-treated spores, heat-killed first then kitalase –treated spores, vinotaste-treated spores, heat-killed spores, pronase E, heat-killed spores then pronase E, UV-treated spores, and resting spores of LCV and LCA strains to stimulate expression of TLR2-CD14 was evaluated. Treating the spores of LCV and LCA strains with kitalase and heat-killed spores following kitalase treatment stimulated the expression of TLR2-CD14. Other treatments were comparable to resting spores of both strains. Data were analyzed by two-way ANOVA and Bonferroni posttest (*** indicates $P < 0.001$, * indicates $P < 0.05$).

resting spores which postulates its role in facilitating the recognition by macrophages. TEM analysis revealed slight alterations of cell wall continuity of the spore surfaces. Absolute ultrastructural alterations could not be determined. This tempts us to conclude that the consequences of episporic modifications take place more in the fungus-macrophage interaction. The current findings are concordant with previous studies that confirmed the capability of macrophages to phagocytose foreign particles depends on size, shape, surface states and morphological characters of the targeted particles [53]. Toll-like receptors (TLRs) have a key role in recognition the fungal pathogens by the innate immune system, in particular for *A. fumigatus* and *C. albicans* as reviewed by van de Veerdonk [54]. Our finding elucidated the stimulation of TLR2 expression after kitalase treatment of *Lichtheimia* spores as it was shown for *Pseudallescheria boydii* and *A. fumigatus* [55]. This finding confirms the role of carbohydrate compartments and its associated

cell wall components in stimulating TLRs after glucan exposure after *endo*-β1.3-glucanolysis. The spore surface components which exactly stimulate the response of TLRs will be studied in the near future. On the host side, heat-shock proteins were shown to be dominant candidates exposed on the surface of macrophages during the interaction with *Lichtheimia* spores, in particular the heat-shock 70 kDa protein 8 (Hspa8) [56]. This study provides proof for spore surface proteins in the recognition of *L. corymbifera* by macrophages and emphasizes the role of surface proteins as key players of the interaction between *L. corymbifera* and macrophages.

5. Conclusions

The current study shows the importance of episporic components of *Lichtheimia* spores in the recognition by macrophages. It sheds light on the role of spore surface proteins of *Lichtheimia* spores during the interaction with macrophages. Therefore, it is necessary to determine the protein candidates that are present on the surface of the cell wall of *Lichtheimia* spores by proteomic analysis and subsequently to investigate the function of the most abundant surface protein candidates during interaction with host cells. All these findings suggest the role of proteins for the host and pathogen sides during the interaction process.

6. Ethics statement

All experiments were performed in compliance with the European and Austrian animal protection law. According to this, no specific approval is needed for work performed in *Galleria mellonella* larvae.

Declaration of Competing Interest

The authors declare that they have no known competing financial interests or personal relationships that could have appeared to influence the work reported in this paper.

Acknowledgement

This study was funded by the German Research Foundation (DFG) through the Collaborative Research Center/Transregio FungiNet 124 'Pathogenic fungi and their human host: Networks of Interaction', DFG project number 210879364, project A3 and A6 to UT and KV, respectively, and by the Federal Ministry of Education and Research (Bundesministerium für Bildung und Forschung [BMBF] grant: FKZ 13GW0245B to RM. We thank Leibniz Science Campus (HotAim) und the German Research Foundation (DFG through the Collaborative Research Center 1278 PolyTarget 'Polymer-based nanoparticle libraries for targeted anti-inflammatory strategies', DFG project number 316213987, project B04 to VD for financial support. We also thank for financial support by the German Egyptian Research Long-term Scholarship (GERLS) Program 2014 (57030312 for MIAH.) coordinated by the German Academic Exchange Service (DAAD). We thank Caroline Hörtnagel (Medical University Innsbruck, Austria) for help with the *Galleria* infection model, Sören Doose (JMU Würzburg, Germany) for fitting the spore germination data with the Baranyi model, Amol Kolte (University Hospital Jena, Germany) as well as Hea-Reung Park and Volker U. Schwartze (FSU Jena, Germany) for technical advice in the initial phase of this study.

Appendix A. Supplementary data

Supplementary data to this article can be found online at https://doi.org/10.1016/j.csbj.2021.01.023.

References

[1] Chander J, Kaur M, Singla N, Punia RPS, Singhal SK, Attri AK, et al. Mucormycosis: battle with the deadly enemy over a five-year period in India. J Fungi 2018;4(2):46. https://doi.org/10.3390/jof4020046.
[2] Gebremariam T, Liu M, Luo G, Bruno V, Phan QT, Waring AJ, et al. CotH3 mediates fungal invasion of host cells during mucormycosis. J Clin Invest 2014;124:237–50. https://doi.org/10.1172/JCI71349.
[3] Liu M, Spellberg B, Phan QT, Fu Y, Fu Y, Lee AS, et al. The endothelial cell receptor GRP78 is required for mucormycosis pathogenesis in diabetic mice. J Clin Invest 2010;120:1914–24. https://doi.org/10.1172/JCI42164.
[4] Hassan MIA, Cseresnyes Z, Al-Zaben N, Dahse HM, Vilela de Oliveira RJ, Walther G, et al. The geographical region of origin determines the phagocytic vulnerability of Lichtheimia strains. Environ Microbiol 2019;21:4563–81. https://doi.org/10.1111/1462-2920.14752.
[5] Platauf AP. Mycosis mucorina. Virchows Arch 1885;102:543–64.
[6] Hoffmann K, Walther G, Voigt K. *Mycocladus* vs. *Lichtheimia*, a correction (*Lichtheimiaceae* fam. nov., Mucorales, Mucoromycotina). Mycol Res 2009;113 (3):277–8.
[7] Alastruey-Izquierdo A, Cuesta I, Walther G, Cuenca-Estrella M, Rodriguez-Tudela JL. Antifungal susceptibility profile of human-pathogenic species of *Lichtheimia*. J Antimicrob Chemother 2010;54:3058–60. https://doi.org/10.1128/AAC.01270-09.
[8] Hassan MIA, Voigt K. Pathogenicity patterns of mucormycosis: epidemiology, interaction with immune cells and virulence factors. Med Mycol 2019;57: S245–56. https://doi.org/10.1093/mmy/myz011.
[9] Schwartze VU, de A, Santiago ALCM, Jacobsen ID, Voigt K. The pathogenic potential of the Lichtheimia genus revisited: Lichtheimia brasiliensis is a novel, non-pathogenic species. Mycoses 2014;57:128–31. https://doi.org/10.1111/myc.12230.
[10] Gordon SB, Read RC. Macrophage defences against respiratory tract infections. Br Med Bull 2002;61:45–61. https://doi.org/10.1093/bmb/61.1.45.
[11] Horn F, Heinekamp T, Kniemeyer O, Pollmächer J, Valiante V, Brakhage AA. Systems biology of fungal infection. Front Microbiol 2012;3:1–20. https://doi.org/10.3389/fmicb.2012.00108.
[12] Andrianaki AM, Kyrmizi I, Thanopoulou K, Baldin C, Drakos E, Soliman SSM, et al. Iron restriction inside macrophages regulates pulmonary host defense against *Rhizopus* species. Nat Commun 2018;9:3333. https://doi.org/10.1038/s41467-018-05820-2.
[13] López-Fernández L, Sanchis M, Navarro-Rodríguez P, Nicolás FE, Silva-Franco F, Guarro J, et al. Understanding *Mucor circinelloides* pathogenesis by comparative genomic and phenotypical studies. Virulence 2018;9(1):707–20. https://doi.org/10.1080/21505594.2018.1435249.
[14] Mukherjee K, Altincicek B, Hain T, Domann E, Vilcinskas A, Chakraborty T. *Galleria mellonella* as a model system for studying *Listeria* pathogenesis. Appl Environ Microbiol 2010;76:310–7. https://doi.org/10.1128/AEM.01301-09.
[15] Schwartze VU, Hoffmann K, Nyilasi I, Papp T, Vágvölgyi C, de Hoog S, et al. *Lichtheimia* Species exhibit differences in virulence potential. PLoS ONE 2012;7:. https://doi.org/10.1371/journal.pone.0040908e40908.
[16] Schulze B, Rambach G, Schwartze VU, Voigt K, Schubert K, Speth C, et al. Ketoacidosis alone does not predispose to mucormycosis by *Lichtheimia* in a murine pulmonary infection model. Virulence 2017;8(8):1657–67. https://doi.org/10.1080/21505594.2017.1360460.
[17] Mohebbi S, Erfurth F, Hennersdorf P, Brakhage AA, Saluz HP. Hyperspectral imaging using intracellular spies: quantitative real-time measurement of intracellular parameters in vivo during interaction of the pathogenic fungus Aspergillus fumigatus with human monocytes. PLoS One 2016;11(e0163505). https://doi.org/10.1371/journal.pone.0163505.
[18] Schindelin J, Arganda-Carreras I, Frise E, Kaynig V, Longair M, Pietzsch T, et al. Fiji: an open-source platform for biological-image analysis. Nat Methods 2012;9:676–82. https://doi.org/10.1038/nmeth.2019.
[19] Brunk M, Sputh S, Doose S, Van De Linde S, Terpitz U. HyphaTracker: an ImageJ toolbox for time-resolved analysis of spore germination in filamentous fungi. Sci Rep 2018;8:605. https://doi.org/10.1038/s41598-017-19103-1.
[20] Oliphant TE. Python for scientific computing. Comput Sci Eng 2007;9:10–20. https://doi.org/10.1109/MCSE.2007.58.
[21] Dierckx P. Curve and Surface Fitting with Splines. New York: Clarendon; 1993.
[22] Volling K, Brakhage AA, Saluz HP. Apoptosis inhibition of alveolar macrophages upon interaction with conidia of *Aspergillus fumigatus*. FEMS Microbiol Lett 2007;275:250–4. https://doi.org/10.1111/j.1574-6968.2007.00883.x.
[23] Hornbach A, Heyken A, Schild L, Hube B, Löffler J, Kurzai O. The glycosylphosphatidylinositol-anchored protease Sap9 modulates the interaction of *Candida albicans* with human neutrophils. Infect Immun 2009;77:5216–24. https://doi.org/10.1128/IAI.00723-09.
[24] Bocklitz T, Kämmer E, Stöckel S, Cialla-May D, Weber K, Zell R, et al. Single virus detection by means of atomic force microscopy in combination with

advanced image analysis. J Struct Biol 2014;188(e0163505):30–8. https://doi.org/10.1016/j.jsb.2014.08.008.
[25] Kämmer E, Götz I, Bocklitz T, Stöckel S, Dellith A, Cialla-May D, et al. Single particle analysis of herpes simplex virus: comparing the dimensions of one and the same virions via atomic force and scanning electron microscopy. Anal Bioanal Chem 2016;408:4035–41. https://doi.org/10.1007/s00216-016-9492-1.
[26] Borcherds W, Theillet FX, Katzer A, Finzel A, Mishall KM, Powell AT, et al. Disorder and residual helicity alter p53-Mdm2 binding affinity and signaling in cells. Nat Chem Biol 2014;10:1000–2. https://doi.org/10.1038/nchembio.1668.
[27] Dull T, Zufferey R, Kelly M, Mandel RJ, Nguyen M, Trono D, et al. A third-generation Lentivirus vector with a conditional packaging system. J Virol 1998;72:8463–71. https://doi.org/10.1128/jvi.72.11.8463-8471.1998.
[28] Chua J, Senft JL, Lockett SJ, Brett PJ, Burtnick MN, DeShazer D, et al. pH alkalinization by chloroquine suppresses pathogenic *Burkholderia* type 6 secretion system 1 and multinucleated giant cells. Infect Immun 2017;85(1): e00586–e616. https://doi.org/10.1128/IAI.00586-16.
[29] Al-Bari MAA. Targeting endosomal acidification by chloroquine analogs as a promising strategy for the treatment of emerging viral diseases. Pharmacol Res Perspect 2017;5(1):. https://doi.org/10.1002/prp2.293e00293.
[30] Janeway CA, Medzhitov R. Innate immune recognition. Annu Rev Immunol 2002;20:197–216. https://doi.org/10.1146/annurev.immunol.20.083001.084359.
[31] Kraibooj K, Park HR, Dahse HM, Skerka C, Voigt K, Figge MT. Virulent strain of *Lichtheimia corymbifera* shows increased phagocytosis by macrophages as revealed by automated microscopy image analysis. Mycoses 2014;57:56–66. https://doi.org/10.1111/myc.12237.
[32] Elieh Ali Komi D, Sharma L, Dela Cruz CS. Chitin and its effects on inflammatory and immune responses. Clin Rev Allergy Immunol 2018;54:213–23. https://doi.org/10.1007/s12016-017-8600-0.
[33] Kovacs-Simon A, Titball RW, Michell SL. Lipoproteins of bacterial pathogens. Infect Immun 2011;79:548–61. https://doi.org/10.1128/IAI.00682-10.
[34] Sit B, Crowley SM, Bhullar K, Lai CCL, Tang C, Hooda Y, et al. Active transport of phosphorylated carbohydrates promotes intestinal colonization and transmission of a bacterial pathogen. PLoS Pathog 2015;11(8):. https://doi.org/10.1371/journal.ppat.1005107e1005107.
[35] Voltersen V, Blango MG, Herrmann S, Schmidt F, Heinekamp T, Strassburger M, et al. Proteome analysis reveals the conidial surface protein CcpA essential for virulence of the pathogenic fungus *Aspergillus fumigatus*. mBio 2018;9(5): e01557–e1618. https://doi.org/10.1128/mbio.01557-18.
[36] Luther K, Torosantucci A, Brakhage AA, Heesemann J, Ebel F. Phagocytosis of *Aspergillus fumigatus* conidia by murine macrophages involves recognition by the dectin-1 beta-glucan receptor and Toll-like receptor 2. Cell Microbiol 2007;9:368–81. https://doi.org/10.1111/j.1462-5822.2006.00796.x.
[37] Granja LFZ, Pinto L, Almeida CA, Alviano DS, Da Silva MH, Ejzemberg R, et al. Spores of *Mucor ramosissimus*, *Mucor plumbeus* and *Mucor circinelloides* and their ability to activate human complement system in vitro. Med Mycol 2010;48:278–84. https://doi.org/10.3109/13693780903096669.
[38] Marx RS, Forsyth KR, Hentz SK. Mucorales species activation of a serum leukotactic factor. Infect Immun 1982;38:1217–22. https://doi.org/10.1128/iai.38.3.1217-1222.1982.
[39] Zipfel PF, Würzner R, Skerka C. Complement evasion of pathogens: common strategies are shared by diverse organisms. Mol Immunol 2007;44:3850–7. https://doi.org/10.1016/j.molimm.2007.06.149.
[40] Kinchen JM, Ravichandran KS. Phagosome maturation: going through the acid test. Nat Rev Mol Cell Biol 2008;9:781–95. https://doi.org/10.1038/nrm2515.
[41] Heinekamp T, Schmidt H, Lapp K, Pähtz V, Shopova I, Köster-Eiserfunke N, et al. Interference of *Aspergillus fumigatus* with the immune response. Semin Immunopathol 2014;37:141–52. https://doi.org/10.1007/s00281-014-0465-1.
[42] Schwartze VU, Winter S, Shelest E, Marcet-Houben M, Horn F, Wehner S, et al. Gene expansion shapes genome architecture in the human pathogen *Lichtheimia corymbifera*: an evolutionary genomics analysis in the ancient terrestrial mucorales (Mucoromycotina). PLoS Genet. 2014;10(8):. https://doi.org/10.1371/journal.pgen.1004496e1004496.
[43] Voigt K, Wolf T, Ochsenreiter K, Nagy G, Kaerger K, Shelest E, Papp T. Genetic and metabolic aspects of primary and secondary metabolism of the Zygomycetes. In: Hoffmeister D, editor. The Mycota Vol. III: Biochemistry and Molecular Biology. Berlin, Heidelberg, New York: Springer Verlag; 2016. p. 361–85. https://doi.org/10.1007/978-3-319-27790-5_15.
[44] Vylkova S, Lorenz MC. Modulation of phagosomal pH by *Candida albicans* promotes hyphal morphogenesis and requires Stp2p, a Regulator of amino acid transport. PLoS Pathog 2014;10(3):. https://doi.org/10.1371/journal.ppat.1003995e1003995.
[45] Ibrahim AS, Skory CD. Genetic manipulation of zygomycetes. Med Mycol: Cell Mol Tech 2007:305–26. https://doi.org/10.1002/9780470057414.ch14.
[46] Nagy G, Szebenyi C, Csernetics Á, Vaz AG, Tóth EJ, Vágvölgyi C, et al. Development of a plasmid free CRISPR-Cas9 system for the genetic modification of *Mucor circinelloides*. Sci Rep 2017;7(1):16800. https://doi.org/10.1038/s41598-017-17118-2.
[47] Yang CL, Wang J, Zou LL. Innate immune evasion strategies against cryptococcal meningitis caused by *Cryptococcus neoformans*. Exp Ther Med 2017;14:5243–50. https://doi.org/10.3892/etm.2017.5220.
[48] Volling K, Thywissen A, Brakhage AA, Saluz HP. Phagocytosis of melanized *Aspergillus* conidia by macrophages exerts cytoprotective effects by sustained pi3k/akt signalling. Cell Microbiol 2011;13:1130–48. https://doi.org/10.1111/j.1462-5822.2011.01605.x.
[49] Shelest E, Voigt K. Genomics to study basal lineage fungal biology: phylogenomics suggests a common origin. In: Nowrousian M, editor. The Mycota Vol III: Fungal Genomics. Berlin, Heidelberg, New York: Springer Verlag; 2014. p. 31–60. https://doi.org/10.1007/978-3-642-45218-5_2.
[50] Kohchi C, Inagawa H, Nishizawa T, Soma GI. ROS and innate immunity. Anticancer Res 2009;29::817–822.
[51] Gersuk GM, Underhill DM, Zhu L, Marr KA. Dectin-1 and TLRs permit macrophages to distinguish between Different *Aspergillus fumigatus* cellular states. J Immunol 2006;176:3717–24. https://doi.org/10.4049/jimmunol.176.6.3717.
[52] Maurer E, Hörtnagl C, Lackner M, Grässle D, Naschberger V, Moser P, et al. *Galleria mellonella* as a model system to study virulence potential of mucormycetes and evaluation of antifungal treatment. Med Mycol 2019;57:351–62. https://doi.org/10.1093/mmy/myy042.
[53] Paul D, Achouri S, Yoon YZ, Herre J, Bryant CE, Cicuta P. Phagocytosis dynamics depends on target shape. Biophys J 2013;105(5):1143–50. https://doi.org/10.1016/j.bpj.2013.07.036.
[54] van de Veerdonk FL, Kullberg BJ, van der Meer JW, Gow NA, Netea MG. Host-microbe interactions: innate pattern recognition of fungal pathogens. Curr Opin Microbiol 2008;11:305–12. https://doi.org/10.1016/j.mib.2008.06.002.
[55] Figueiredo RT, Carneiro LAM, Bozza MT. Fungal surface and innate immune recognition of filamentous fungi. Front Microbiol 2011;2:1–14. https://doi.org/10.3389/fmicb.2011.00248.
[56] Hassan MIA, Kruse JM, Krüger T, Dahse H, Cseresnyés Z, Blango MG, et al. Functional surface proteomic profiling reveals the host heat-shock protein A8 as a mediator of *Lichtheimia corymbifera* recognition by murine alveolar macrophages. Environ Microbiol 2020;22(9):3722–40. https://doi.org/10.1111/1462-2920.15140.